INTRA-TUMORAL DRUG METABOLISM: EVALUATING THE IMPACT OF UGT OVEREXPRESSION ON ANTICANCER DRUG EFFICACY IN BREAST CANCER

By

Sandra George

Master Of Biotechnology

Thesis

Submitted to Flinders University

for the degree of

Master of Biotechnology

College of Medicine and Public Health

2nd June 2025

TABLE OF CONTENTS

LIST OF FIGURES

LIST OF TABLES

DECLARATION

I certify that this thesis: does not incorporate without acknowledgment any material previously submitted for a degree or diploma in any university and the research within will not be submitted for any other future degree or diploma without the permission of Flinders University; and to the best of my knowledge and belief, does not contain any material previously published or written by another person except where due reference is made in the text.

Sandra George

2nd June 2025

ACKNOWLEDGEMENT

I would like to express my appreciation to all individuals who guided and supported me throughout the period of this research study and completion of master's thesis.

Most importantly, I am sincerely thankful to my incredible supervisor, Dr. Robyn Meech, for her unwavering guidance, keen supervision and inspiration throughout the project. Her expertise and mentorship have played a pivotal role in the formation of this research as well as my growth as a biotechnology scientist. I'm truly indebted to your endless kindness you have shown towards me and your work ethic have instilled values that I will cherish throughout my professional path.

I also appreciate the members of the research lab. Thankful to Emeritus Professor Peter Mackenzie, for the honest suggestions and constructive criticisms. Your broad understanding about the cancer research is admirable. Special thanks to lab manager, Alex for making it possible with the timely availability of the materials required for the project. PhD student, Dylan Martin for the support in data analysis advice and for always being available to help at my stuck points.

I would like to extend my thanks to previous members of Prof. Meech's lab, as their works have helped shaped the current study. Particularly, Mr. Quinn Martin for the generation of the stable cell lines used in the study. Findings from independent research conducted by Dr. Radwan Ansaar has contributed to the formulation of some parts of the project.

I also want to thank Flinders university, FHMRI and HMRB for giving me the facilities and resources needed for conducting the study, as well as administration staff for their coordination in training and technical things.

This project was conducted for the completion of master's course in Biotechnology under the College of Medicine and Public Health which was overseen by course coordinator Dr. Alistair Standish. I extend my appreciation for his advice and guidance in completion of this thesis.

A heartfelt thanks to my friends and family for being patient with me, supportive and believing in me, especially during difficult period of this endeavour. Especially, my partner, Bibin Pulickal, and my baby, Serin Pulickal who provided me with infinite love and greatest motivation to achieve the completion of this project.

Thankful to everyone who contributed in some grand way or small way.

LIST OF ABBREVIATIONS

µL	Microlitre
µM	Micromolar
4-OH TAM	4-hydroxytamoxifen
ADME	Absorption Distribution Metabolism Excretion
AML	Acute Myelogenous Leukemia
AR	Androgen receptor
ATCC	American Type Culture Collection
BC	Breast cancer
Bp	Base Pairs
cDNA	complementary Deoxyribonucleic acid
Ct	Cycle Threshold
CYP2D6	Cytochrome P450 2D6
DHT	Dihydrotestosterone
DME	Drug Metabolising Enzymes
DMEM	Dulbecco's Modified Eagle's Medium
dNTP	Deoxy Nucleotide Tri Phosphate
E2	Estradiol
EDTA	Ethylene di amine tetra acetic acid
ER	Estrogen Receptor
FBS	Foetal Bovine Serum
FDA	Food and Drug Administration
GREB1	Growth Regulation by Estrogen in Breast cancer 1

HER	Human epidermal growth receptor 2
HMRB	Health Medical Research Building
IBC	Institutional Biosafety Committee
Kb	Kilobase
kDa	Kilo Daltons
mM	Millimetre
mRNA	messenger ribonucleic acid
nm	Nanometre
nM	Nanomolar
NTC	Negative Template Control
PBS	Phosphate Buffered Saline
PC2	Physical containment level 2
PCR	Polymerase Chain Reaction
PPE	Personal protective equipment
PR	Progesterone Receptor
qRT-PCR	quantitative Reverse Transcription Polymerase Chain Reaction
RNA	Ribonucleic Acid
RPMI	Roswell Park Memorial Institute Medium
RT	Reverse Transcription
SARM	Selective androgen receptor modulators
SDS-PAGE	Sodium Dodecyl Sulphate Polyacrylamide Gel Electrophoresis
SERD	Selective estrogen receptor degraders
SERM	Selective estrogen receptor modulators
SF	Serum Free

SNP	Single nucleotide polymorphisms
TAM	Tamoxifen
TCGA	The Cancer Genome Atlas
TNBC	Triple-negative breast cancers
UGT	Uridine 5'-Diphospho-Glucuronosyltransferase
USA	United States of America
UV	Ultra-violet

ABSTRACT

Breast cancer is one of the most prevalent cancers in which the treatment efficacy is reduced due to drug resistance. Estrogen receptor positive breast cancer is commonly treated with tamoxifen; however up to 40% of patients develop resistance to the drug. Here, it was examined whether overexpression of a specific member of the drug metabolising enzyme family, Uridine 5'-Diphospho-Glucuronosyltransferase (UGT) changes the sensitivity of MCF7 breast cancer cells to 4-hydroxytamoxifen (4-OH-TAM), which is the active form of the drug. Two paradigms were established, the first used short term (transient) overexpression of UGT2B15 and the second used long term (stable) overexpression of UGT2B15. MCF7 cells that were transiently transfected with UGT2B15, or control plasmids, were treated with varying doses of 4-OH-TAM, and cell proliferation measured via the crystal violet method. Cells over-expressing UGT2B15 showed resistance to 4-OH-TAM induced growth inhibition, with the effect statistically significant at low doses of the drug. Analysis of estrogen stimulated PS2 gene expression in MCF7 cells revealed that pretreatment of 4-OH-TAM reduced E2-mediated PS2 induction in control cells and UGT2B15 overexpressing cells alike. These differences were not statistically significant, likely due to high variance between the replicate experiments. To study the effects of UGT2B15 on long-term 4-OH-TAM response, cells with stably integrated UGT2B15 or control plasmids were modified by integration of green and red fluorescent protein reporter plasmids. The overexpression of UGT2B15 was confirmed by immunoblot and expression of fluorescent proteins was confirmed by microscopy. These ‘double-stable’ cells lines were used to establish a competitive growth assay. A pilot study showed that microscopy could be used to quantify the relative growth of labelled cells; however preliminary data was not sufficient to conclude whether UGT2B15 provided a long-term drug-specific growth/survival advantage. Collectively, these results suggest that while UGT2B15 has potential to impart resistance to low doses of 4-OH-TAM in vitro, further studies are required to determine the dose-dependence of this effect, and whether it translates to more natural tumour-like models that include cell-type heterogeneity. These findings are representative of the multidimensionality of tamoxifen resistance mechanism and lend further stimulus for investigation in clinical importance of UGT2B15 in cancer therapy.

1 INTRODUCTION

Breast cancer (BC) (Glaser & Dimitrakakis, 2013) is a prevalent disease affecting 1 in 7 women over their lifetime. It is the second most commonly diagnosed cancer among females in Australia (National Breast Cancer Foundation, 2024). The complexity of treating breast cancer is increased by the problem of drug resistance, which describes a situation where tumours either never respond to the drug, or they initially respond but then lose response to the drug over time. There are many mechanisms for drug resistance; one of which is metabolism of anticancer drugs within the tumour cells (Akhdar et al., 2012). This project studies the role of UDP-glucuronosyltransferases (UGTs) in intratumoral drug metabolism. In particular, the focus is on the roles of a UGT enzymes called UGT2B15, in determining the efficacy of hormonal therapies which are used to treat the most common subtypes of BC which express the estrogen receptor (Hu et al., 2016). The overexpression of UGT2B15 presents a significant area for exploration, as it may directly influence patient outcomes. Continued research is essential to unravel the complexities of tumour metabolism and its implications for therapeutic strategies in breast cancer treatment.

This review summarizes the role of tamoxifen in breast cancer treatment, various studies that examined the role of UGTs in drug metabolism and other previous findings relating to this intratumoral drug metabolism. This review will then identify gaps in our understanding which will lead to the development of the hypotheses and aims of this project. The results from this project could eventually be used to tailor strategies to overcome drug resistance leading to more effective treatment approaches.

1.1 Breast cancer and treatment approaches

Breast cancer remains one of the most prevalent and challenging malignancies worldwide (Perou et al., 2000). In 2018, it ranked as the second highest cause of cancer-related diagnoses globally, with 2.1 million new cases accounting for 11.6% of total cancer cases, second only to lung cancer and ahead of prostate cancer (Bray et al., 2018). Among women, breast cancer was the leading cause of cancer diagnoses, representing 24.2% or approximately 1 in 4 new cancer cases worldwide (WHO, 2018). The disease's impact is further underscored by an estimated 627,000 women who died from breast cancer in the same year, accounting for 15% of female cancer deaths globally. In the United States, the National Cancer Institute estimates breast cancer to be the leading non-melanoma cancer cause, with over 281,000

estimated cases in 2021, representing 14.8% of all new cancer cases (Wang & Wu, 2023). These statistics highlight the significant burden of breast cancer on global health and emphasize the need for continued research and improved treatment strategies.

Breast cancers are categorized by hormone-dependent or hormone-independent status, which informs oncologists about typical tumour characteristics and response to specific treatments. The heterogeneity of breast cancers is further represented by molecular subtyping based on the expression and mutations of multiple hormone receptor genes (Orrantia-Borunda et al., 2022; Waks & Winer, 2019). Healthy breast tissue depends on multiple hormones signalling pathways to maintain cell homeostasis and proliferation. Mutation or loss of expression of these receptors may convey hormone independence, limiting available treatment options for patients. In order to direct treatment, patient biopsies are examined for the expression of two steroid hormone receptors: estrogen receptor alpha (ERα) and progesterone receptor. ERα is a growth promoting receptor that drives the expression of many pro-proliferative genes in response to binding the steroid hormone estrogen. PR is a direct downstream target of ERα, and its expression provides evidence that the ER is active in the cells. Tumours that have expression of the hormone receptors ERα and PR can be treated with hormonal therapies that target the ER (Hu et al., 2016). In addition, biopsies are examined for the expression and mutational status of the growth factor receptor called human epidermal growth receptor 2 (HER2) (Hunter et al.). Tumours that show amplification of the HER2 gene can be treated with anti-HER2 therapies such as Herceptin (Waks & Winer, 2019). Triple-negative breast cancers (TNBC) are defined as those that lack expression or activity of all three of these receptor pathways (ER-, PR-, HER2-) (Gonçalves et al., 2018). TNBC have more aggressive tumour characteristics and have fewer treatment options (Yang et al., 2007). In general TNBC patients are treated with cytotoxic chemotherapy which also has more adverse effects than hormonal and HER2-targeted therapies (Wang & Wu, 2023). In some cancers, dysregulation of these receptor pathways and other growth-promoting genes leads to excessive signalling, resulting in aberrant hormone receptor signalling that dysregulates cell homeostasis and allows auto-regulatory positive feedback loops to drive cancer growth.

About 70 to 80 per cent of breast cancers are termed hormone receptor-positive because they express both the ERα and PR (ER+/PR+) (Orrantia-Borunda et al., 2022). The gold standard treatment for ER+/PR+ breast cancer utilises hormonal (endocrine) therapies, particularly selective estrogen receptor modulators (SERMs), aromatase inhibitors, and/or selective estrogen receptor degraders (SERDs) (Rozeboom et al., 2019). SERMs are estrogen-

like chemicals that have the capacity to either activate or inhibit the function of the ER when it binds to different target gene, which is due largely to recruitment of different transcriptional co-factors (Harrington et al., 2006). SERMs revolutionised targeted treatment of ER+/PR+ breast cancer because they provide tissue-specific inhibition of the ERα whilst minimising adverse effects on other estrogen-responsive tissues. Since FDA approval in 1985, Tamoxifen (Gonçalves et al.) has been one of the most widely used SERM therapies (Kisanga et al., 2004) and has significantly improved hormone responsive breast cancer patient outcomes since its approval (Rozeboom et al., 2019). TAM most likely benefit patients with ER+ tumours (Farrar & Jacobs, 2024). In breast tissue, tamoxifen inhibits the actions of endogenous estrogens through competitively binding to the ERα (e.g. acts as an ERα -antagonist). This leads to inhibition of breast cancer cell growth. In contrast, in some other estrogen-responsive tissues, such as bone, tamoxifen either does not block ERα activity or can activate the ER (e.g. act as an ERα -agonist) (Farrar & Jacobs, 2024). However, it is also important to note that even in breast tissues, some genes are repressed by the action of tamoxifen while others are activated. Tamoxifen itself has relatively poor affinity for ERα and instead acts as a prodrug for more potent anti-hormonal metabolites, namely 4-hydroxy-N-desmethyl-tamoxifen (endoxifen) and 4-hydroxytamoxifen (4-OH-TAM) (Chanawong et al., 2015). Cytochrome P450 2D6 (CYP2D6) is mainly responsible for conversion of tamoxifen into active forms (Krauß & Bracher, 2018; Lazarus et al., 2009). As will be discussed in section 1.5, the active forms are subsequently inactivated by specific UDP-glucuronosyltransferase enzymes.

Currently, the status of the androgen receptor (AR) expression in breast tumours is not assessed as part of the standard clinical analysis of tumour biopsies. However, it is known that around 80% of ER+/PR+ breast tumours also express the AR (AR+). In addition, recent data indicates that AR expression in these tumours is a positive prognostic signal because the AR may be able to antagonise the activity of the ERα. Building on this information, an emerging modality for ER+/PR+ breast cancer that may one day serve as an alternative to anti-estrogen therapies such as Tamoxifen, is treatment with androgens or selective androgen receptor modulators (SARMs). Studies in vitro using various ER+/AR+ breast cancer cell models including cell lines and patient-derived explants, have shown that androgens can indirectly inhibit ERα by activating an AR and that this can be effective in blocking cell proliferation (Hickey et al., 2021). This strategy has recently advanced to a small Phase 2 clinical trial of breast cancer patients with ER+ and AR+ breast tumours that had advanced after treatment with standard hormonal therapies (Palmieri et al., 2024). In this trial the researchers concluded

that activating the AR using an androgen or SARM could result in clinical benefit for some patients that are no longer receiving benefit from other treatments due to drug resistance (Palmieri et al., 2024). Based on this study, it is proposed that selective AR activation should be further investigated as a new clinical approach, particularly for ER+ patients who do not respond to standard hormonal therapies such as Tamoxifen.

1.2 Research models for studying the effects of different hormonal therapies on ER+ breast cancer

In vitro research on breast cancer utilizes cancer cell line models representative of different breast cancer subtypes and receptor status. These include mammary epithelium cells that are ER+ particularly MCF-7 and ZR-75. These cell lines provide valuable tools for investigating the molecular mechanisms underlying breast cancer progression and treatment response. MCF7 and ZR75 cells express ERα but represent different types of ER+ breast cancer models, with MCF-7 cells having a lower AR/ER ratio than ZR-75 cells. In addition, previous work in this laboratory showed that the cell lines have different responses to both estrogen and androgen treatment. Specifically, a series of experiments were performed in which both cell lines were treated with either a potent estrogen (Estradiol, E2), a potent androgen (dihydrotestosterone, DHT), or a combination of both, and the effects on growth were studied. It was found that E2 increased growth of MCF7 cells but did not increase growth of ZR75 cells. This indicates that only MCF7 cells are a good model for breast cancer types in which estrogen stimulates growth. This is also consistent with other published studies that show that estrogen stimulates the growth of MCF7 cells and that anti-estrogens including tamoxifen inhibit growth of MCF7 cells. When both cell lines were treated with DHT, it was found that the androgen completely blocked growth of ZR75 cells but only moderately reduced growth of MCF7 cells. When both E2 and DHT were applied simultaneously, the growth of ZR75 cells was still completely blocked. This indicated that DHT antagonizes growth even when there is estrogen present in the growth media. This suggested that ZR-75 is a good model for breast cancer types in which androgen therapy may be able to reduce growth by antagonising estrogen activity. Finally, when E2 and DHT were applied simultaneously to MCF7 cells, there was no inhibition of growth relative to treatment with E2 alone. This indicated that DHT cannot antagonize estrogen-stimulated growth in this cell line. This suggested that MCF7 is not a good model for

breast cancer types in which androgens may be able to reduce growth by antagonising estrogen activity.

Based on the information about how these different cell lines respond to estrogens and androgens, it was decided that studies that require the analysis of Tamoxifen sensitivity would be best performed in MCF7 cells because they show a pro-proliferative response to estrogen and other literature has shown that their growth can be inhibited by tamoxifen (Hassan et al., 2018; Lippman et al., 1976). In contrast, studies that relate to the analysis of androgen (DHT) sensitivity would be best performed in ZR-75 cells.

1.3 Drug metabolism

In molecular pharmacology, drug metabolism is of interest as variations in expression or function of drug metabolising enzymes have been shown to significantly influence drug disposition (Walsh et al., 2014). Biotransformation of drugs in liver is the most studied area as it typically has the largest effect on systemic drug clearance and thus on overall drug exposure (Yurchenko et al., 2023). However, drug metabolism can also occur locally in target tissues, and this may alter local exposure and hence the drug's efficacy.

Pharmacology is the study of how drugs interact with living systems, encompassing two fundamental concepts: pharmacodynamics and pharmacokinetics. These two aspects are crucial for understanding drug action, efficacy, and safety. Pharmacodynamics focuses on the biochemical and physiological effects of drugs on the body (Marino et al., 2025). It examines how drugs interact with specific molecular targets to elicit therapeutic responses and potential adverse effects. The magnitude of a drug's effect is determined by its ability to engage with and modulate these targets. Pharmacodynamic actions can include modulation of receptor signalling cascades, interaction with enzyme targets, alteration of ion channel and transporter function, influence on hormone systems, effects on structural proteins. These interactions can lead to both intended therapeutic outcomes and unintended side effects. Some effects may be direct results of drug-target interactions, while others may be indirect consequences of altered physiological processes. Pharmacokinetics, on the other hand, describes how the body processes a drug. This is often conceptualized using the ADME principle (Craig, 1998). Absorption: The process by which a drug enters the bloodstream, which varies depending on the route of administration. Distribution: The dispersion of the drug throughout various tissues

in the body, including its target sites. Metabolism: The biochemical transformation of the drug by drug-metabolizing enzymes (DMEs) (Kaur et al., 2020). These reactions can activate or inactivate the compound and often facilitate its excretion. Metabolism occurs in the liver, with secondary sites including the kidneys and gut. Excretion: The elimination of the drug and its metabolites from the body. The primary route is typically via the kidneys, although some drugs are predominantly excreted in faeces, and other minor routes exist. Understanding both pharmacodynamics and pharmacokinetics is essential for predicting drug efficacy, optimizing dosing regimens (Craig, 1998), and anticipating potential drug interactions and adverse effects. The interplay between these two aspects of pharmacology determines the overall therapeutic profile of a drug and guides its clinical use.

Drug metabolism is generally divided in two phases known as Phase I and Phase II. Phase I drug metabolism typically involves reduction, oxidation or hydrolysis reactions that tend to make lipophilic chemicals more polar by creating or exposing a polar functional group. Phase II reactions involve attaching a bulky polar group, such as a sugar or sulphate group, to make the compound even more polar and hence water soluble (Phang-Lyn & Llerena, 2024). The conjugated groups may also provide a negative charge that assists in interaction with anionic transporters thus increasing efflux from the cell.

Figure removed due to copyright restriction.

Figure 1. **Drug metabolism in liver exhibiting the phase II drug metabolising enzymes**

(A) Schematic illustration of hepatic drug metabolism pathway. Here, UGTs perform glucuronidation to detoxify the drug. Drugs are transported into the hepatocyte by influx or efflux drug transporters which are then metabolised by through phase I metabolism that produce metabolites which are subsequently modified by phase II metabolising enzymes. Final metabolites are exported out by efflux transporters.

(B) Schematics displaying phase II glucuronidation reaction facilitating the influx of drug via drug transporters. Drugs are imported into the cell through influx transporters and are subsequently conjugated with UDP-glucuronic acid by UGT enzymes located on the

endoplasmic reticulum to produce inactive drug metabolites. The glucuronidated products are exported out of the cell through efflux transporters.

1.4 UGTs and their role in drug metabolism

UGTs are a superfamily of phase II drug metabolising enzymes that drive the metabolism of various lipophilic chemicals (Pathania et al., 2018). These include xenobiotics such as drugs and environmental chemicals (many of which may be toxic), and endobiotic chemicals including byproducts of normal metabolism and lipophilic signalling molecules such as steroid hormones (Bock, 2016). UGTs mediate the clearance of these diverse chemicals by coupling a sugar group called glucuronic acid to them in a process called glucuronidation (Liu et al., 2023). UGT enzymes are highly expressed in the liver where they act as part of the bodies 'chemical defence' system (Allain et al., 2020; Andrew Rowland et al., 2013; Tukey & Strassburg, 2000). Many of the chemicals that enter the systemic circulation are glucuronidated by hepatic UGTs as blood passes through the liver and the chemicals are taken up into the liver cells (hepatocytes) (Court, 2010). Once they are glucuronidated, the chemicals are more water soluble and more likely to be eliminated via the kidneys. This systemic detoxification mechanism lowers levels of these chemicals in circulation and thus reduces the amount available to enter tissues (A. Rowland et al., 2013). In addition to the liver, UGTs are also expressed in many other tissues where they can mediate local tissue-specific drug metabolism/inactivation. They are commonly expressed in tumours where they can affect the level of drugs within tumour (i.e. intratumoral drug exposure) (Court, 2010; Sutherland et al., 1993).

The mutation and/or differential expression of UGTs can lead to altered pharmacokinetics, affecting drug availability both systemically and within tumour environments. This biotransformation plays a major role in elimination of by-products and regulates the level of many endogenous signalling molecules, which can affect the behaviour of cells and tissues (Meech et al., 2019). Research by Walsh et al. (2014) throws light on the impact of UGT on therapeutic outcomes in breast cancer patients.

There are 22 UGT genes in humans, each encoding different enzymes, that are divided into families and subfamilies called family 1A, 2A and 2B, 3A and 8A (Allain et al., 2020; Liu et al., 2022). Each UGT enzyme metabolizes a different but overlapping range of drugs and

other exogenous and endogenous chemicals. Multiple UGT enzymes are expressed in both normal breast tissue and breast cancer cells. The most reported UGT isoforms in breast tissue include UGT1A1, UGT1A3, UGT1A4, UGT1A6, UGT1A8, UGT1A9, UGT1A10, UGT2B7, UGT2B15, and UGT2B17 (Meech et al., 2019).

Comprehensive analysis of 33 different cancer types showed widespread expression of UGT genes in cancers, with cancer-specific expression profiles. Cancers derived from drug-metabolizing tissues (liver, kidney, gut, pancreas) expressed the largest number of UGT genes (Hu et al., 2021). Several UGT genes were found to be up- or down-regulated in specific cancer types relative to normal tissues. Analysis of 10,069 tumours from 33 cancer types identified 3,427 somatic mutations in UGT genes. About 65% of these mutations were predicted to code for variant UGT proteins with no or reduced activity. These mutations may reduce the capacity of cancer cells to metabolize anti-cancer drugs and pro/anti-cancer endobiotic (Hu, Marri, et al., 2022), potentially altering therapeutic efficacy and cancer growth.. In addition to showing genetic variation that may affect the function of the encoded enzymes, UGT genes also show considerable variation in expression levels in tumours. A recent study found that some UGTs are over expressed in some cancers relative to the corresponding normal tissue(Liu et al., 2022). As discussed in section 1.6 and 1.7, differential expression of UGTs in cancer could affect the levels of chemicals that influence cancer progression (such endogenous growth promoting molecules) and also affect the levels of anti-cancer drugs within tumours.

UGT2B15 and UGT2B17 are of considerable interest in breast cancer. These two enzymes are closely related (see Figure 2) and have similar substrate preferences. Both UGT2B15 and UGT2B17 recognize chemicals that have steroid structures, but they are not equally active with all steroids. The natural most steroids relevant to breast cancer are estrogens and androgens, and steroidal drugs most relevant are SERMs (which have a similar structure to estrogen) and some aromatase inhibitors. Both UGT2B15 and UGT2B17 glucuronidated androgens, but UGT2B17 has higher activity with the most potent androgens, testosterone and dihydrotestosterone (DHT) (Hu et al., 2016) and plays the greater role their elimination. Both UGT2B15 and UGT2B17 also glucuronidated tamoxifen active metabolites but the activity of UGT2B17 is low while the activity of UGT2B15 is high. In this laboratory, the role of these two UGT enzymes in controlling the activity of SERMs and androgens in breast cancer is an ongoing project (Meech et al., 2018).

Figure removed due to copyright restriction.

Figure 2. **UGT Family tree showing 22 human UGT isoforms and its alternative isoforms**.

Dendrogram showing 22 UGT enzyme's isoforms present in human body grouped by subfamily and family. Most of the UGTs have hepatic expression while many also have extrahepatic expression, a reflection of diverse roles in the disposition of drugs and endogenous substrates. Red dots indicate liver biased isoforms and blue dots indicate extrahepatic expression. The green box indicates the main UGT of interest in the current study. [Adapted from (Allain et al., 2020)].

1.5 UGT Expression and cancer progression

UGT2B15 and UGT2B17 genes are both expressed in ER+/AR+ breast cancers and cell lines. They are also both up-regulated by estrogen and androgen, as measured by increased mRNA levels, in a time- and dose-dependent manner. This occurs directly through binding of the ER and AR to the promoters of these two UGT genes (Hu et al., 2016). Moreover, a study from this laboratory showed that tamoxifen and its active tamoxifen metabolites (such as 4-OH TAM) acted as positive regulators of the UGT2B15 gene by agonism (i.e. activating) of the ERα.

Overall, these finding indicate that levels of estrogens, SERMS, and androgens within breast cancer cells could affect the amount of UGT2B15 and UGT2B17 expression, which in turn could affect the levels of specific substrates of these UGTs within the cells. Because these substrates include active tamoxifen metabolites (such as 4-OH TAM) and androgens, this can create feedback loops.

A hypothesis that has influenced the design of this project is that a Tamoxifen-UGT2B15 feedback loop exists in which active tamoxifen metabolites upregulate UGT2B15 expression (Meech et al., 2018) and in turn, UGT2B15 glucuronidates the tamoxifen metabolites leading to their inactivation, which may lower the efficacy of tamoxifen treatment over time. Similarly, it is hypothesized that an androgen-UGT2B17 feedback loop exists in which androgens upregulate UGT2B17 expression, while in turn UGT2B17 inactivates androgens through glucuronidation (Hu et al., 2016). This may lower the efficacy of androgen therapy over time.

Figure removed due to copyright restriction.

Figure 3. **Roles of UGTs in cancer metabolism and drug resistance**

(A) The "glucuronidation metabolic pathway". This reaction plays an important process for metabolism and excretion of a large number of substances, as indicated in left panel. Endogenous metabolites, carcinogens, anticancer agents are brought into or biosynthesised inside the cell. These are then acted upon by UGT enzymes in the endoplasmic reticulum which catalyse the transfer of glucuronic acid from UDP-glucuronic acid to the substrate depicted as 'G'. The result is creation of glucuronides conjugated with 'G' followed by inactivation/elimination from the cell.

(B) Effects of UGTs on various stages of cancer from initiation to progression and relapse due to loss of anti-cancer drug response [Adapted from (Allain et al., 2020)].

(a) Metabolic homeostasis – UGT in normal cells protects them from metabolic homeostasis. Oncogenic pathways tend to interfere with this process.

(b) Modified UGT expression – altered expression of UGT in tumours may be responsible for disrupted endogenous metabolism favouring progression of disease.

(c) Drug mediated UGT induction – when in relapsed/refractory disease, drug mediated induction of UGT can occur. Amplified UGT activity results in inactivation of drug leading to resistant disease and hence contributes to drug resistance.

1.6 Evidence for the impact of intratumoral UGT expression on drug efficacy

Several studies have been conducted to explore the role of metabolic modulation role in enhancing anticancer drug efficacy. For instance, Martorana et al. (2021) investigated the potential of AKT inhibitors in breast cancer treatment, suggesting that targeting metabolic pathways could improve therapeutic responses. Similarly, Saini and Yang (2018) provided insight into the use of metformin as an anti-cancer agent, highlighting its actions in targeting cancer stem cells and its potential to interact with metabolic pathways. However, many of these studies relate to indirect effects of altering general cell metabolism, and not the specific metabolism of the anti-cancer drug itself. This laboratory has focused on drug metabolic enzymes, mainly UGTs, that have capacity to directly inactivate the drug within cancer cells.

To date there have been only a relatively small number of studies that have examined whether UGT-mediated metabolism of drugs can affect the response of cancers to their activity. In discussing how UGT enzymes might affect drug responses it is important to consider that UGTs affect both the systemic and local disposition of drugs as discussed in section 1.5. In the case of anti-cancer drugs, there is evidence that UGTs can affect their efficacy by both mechanisms, i.e. both systemic clearance through glucuronidation in the liver, and local clearance through intratumoral glucuronidation. As an example of the former, studies found that variations in the UGT1A1 gene sequence (single nucleotide polymorphisms, SNPs) alter

glucuronidation of the anti-cancer drug irinotecan, affecting drug levels and increasing adverse effects in patients (Dean, 2012).

Studies that have examined how levels of UGT expression within tumours affect drug responses can be grouped into two types: in vitro and in vivo studies. The in vitro studies include a report that increased levels of UGT2B7 enzyme in melanoma cell lines lead to resistance to the anticancer drug epirubicin. This effect is considered to be direct because UGT2B7 glucuronidates epirubicin. An in vivo study found that high levels of UGT1A gene expression in the leukemic cells of patients with acute myelogenous leukemia (AML) was associated with resistance to the standard treatment of ribavirin and cytarabine. It was subsequently found that the UGTs could glucuronidate ribavirin and cytarabine, which explains the association with outcomes (Zahreddine et al., 2014).

To date there are few published studies investigating how UGT expression in breast cancer cells might affect their sensitivity to anticancer drugs. One study reported that glucuronidation was among the top pathways enriched when MCF7 breast cancer cell line was treated continuously with Tamoxifen; although UGT2B15 was not among the differentially expressed genes reported. One direct approach that has been used in our laboratory to test the role of specific UGT enzymes in promoting resistance to specific anti-cancer drugs is over-expression models. Unpublished work from this laboratory has found that overexpressing UGT2B7 in a breast cancer (TNBC) cell line model increased resistance to epirubicin. This result is consistent with the previously published study performed in a melanoma model. Similar approaches have recently been used in this laboratory to test how the expression levels of UGT2B15 and UGT2B17 enzymes could affect the sensitivity of cancer cells to active tamoxifen metabolites, and androgens, respectively (Martin). This thesis project extends on these studies.

1.7 UGTs as potential biomarker for breast cancer therapy

The expression of specific UGT genes has been associated with patient survival in various cancers, highlighting their potential as prognostic biomarkers. Pharmacogenomic testing of UGT profiles in patients could provide useful prognostic and predictive information (Allain et al., 2020). Clinical studies have provided evidence supporting the role of UGT overexpression in drug resistance (Gao et al., 2013) however, to date many of the studies examine UGT genetic polymorphisms rather than within tumour expression levels.

The cancer genome atlas (TCGA) project has collected transcriptome data for large cohorts of patients with various cancers by performing RNA-seq on tumour biopsies. It also collects clinical data such as survival metrics (Institute). This makes it an excellent tool for studying how the expression levels of specific genes within tumours may be associated with clinical outcomes. In prior work in this laboratory, the expression of various UGTs were examined in the TCGA breast cancer dataset (TCGA-BRCA) dataset. For UGT2B15, the association of expression with survival was examined in cohorts that were treated with tamoxifen, or with other drugs. Some of this analysis is depicted in figure 4 which shows that high intratumoral UGT2B15 expression correlates with reduced disease-free survival, specifically in the cohort of ER+ breast cancer patients treated with Tamoxifen (high UGT2B15- expressing patients relapse earlier). There was no association of UGT2B15 expression levels with survival in ER-positive patients treated with a different drug (anastrozole) that is not metabolized by UGT2B15 (not shown). This suggests that UGT2B15 may be an important modulator of Tamoxifen efficacy in patients. However, no experimental models have been reported in literature to test this hypothesis.

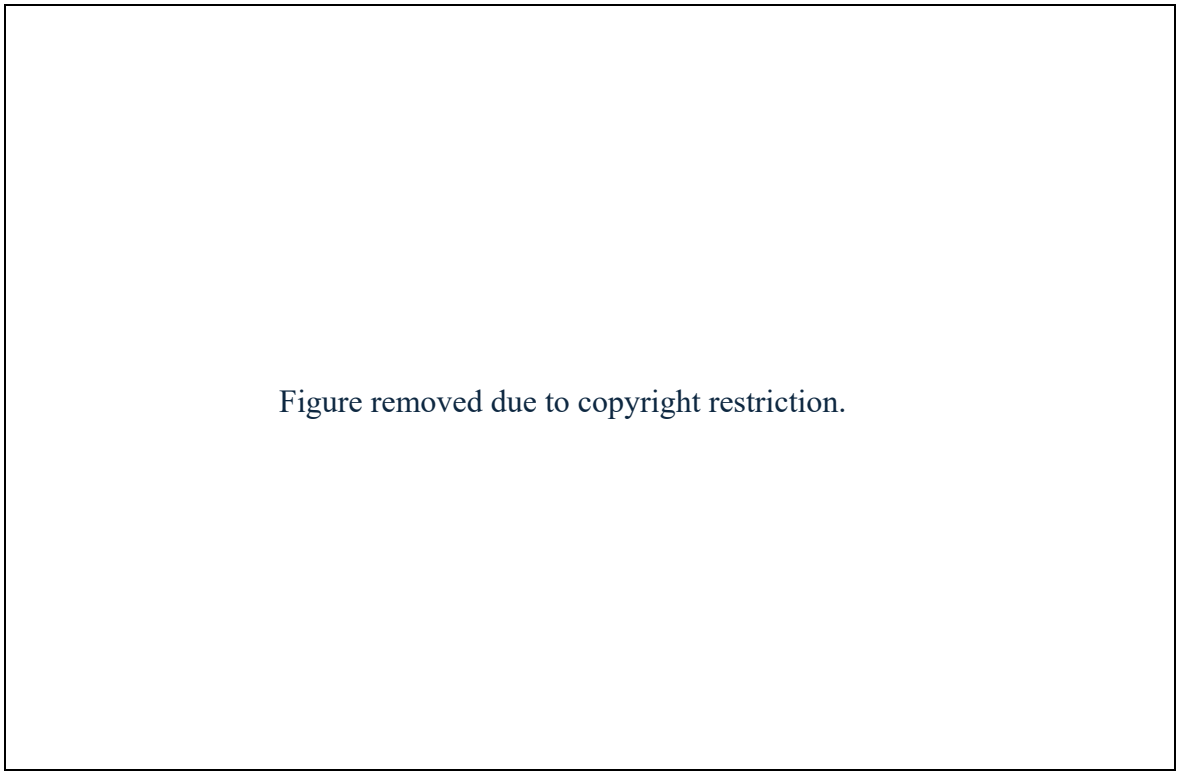

Figure 4. **Disease free survival curve of TAM treated patients stratified by UGT2B15 expression quartiles from the TCGA database**

Kaplan Meier plot displays disease free/progression free survival proportions versus time in months for a cohort of 244 TAM treated patients. The patients were stratified into 4 expression groups/quartiles as A, B, C, D colour coded with blue, red, orange, and green respectively. (https://www.cancer.gov/ccg/research/genome-sequencing/tcga)

(A) Refers to the lowest quartile of UGT2B15 expression (0-4.40)

(B) Refers to the second quartile of UGT2B15 expression (4.58-16.72)

(C) Refers to the third quartile of UGT2B15 expression (16.75-68.97)

(D) Refers to the highest quartile of UGT2B15 expression (72.23-1938.90)

A log rank test P-value of 0.0049 highlights that there is a statistically significant difference in disease free survival among the different quartiles shown. Individuals in quartile D having lower 2B15 expression have a worse prognosis than those with higher expression (Cerami et al., 2012).

In addition to their potential use as biomarker, UGT functional characterisation may identify these enzymes as potential targets of drugs. Other enzymes involved in steroid biosynthesis and biotransformation (e.g. aromatase which converts androgens to estrogens, and 5α reductase that converts testosterone to more potent DHT) are already drug targets in hormone-dependent cancers. Given the intrinsic heterogeneity of breast cancer tumours and their responsiveness to various therapies, the use of more than one therapy has led to improved patient outcomes. Therefore, manipulating steroid-pathways via UGTs might have compounding efficacy when used in a multi-pathway targeting strategy in BC patients.

1.8 Research Rationale

Breast cancer remains one of the prevalent cancers worldwide and despite advancements in treatments, drug resistance continues to be a challenge. Understanding the mechanism of drug resistance becomes a crucial area of research for improving patient care. Combining the literature showing UGTs as a key player in inactivating the anticancer drugs by the process of glucuronidation, and both published and unpublished data from this laboratory, it can be inferred that the overexpression of specific UGT (e.g. UGT2B15) can effect on the intratumoral inactivation/clearance of the drugs used to treat ER+ (or ER+/AR+ BC) Meech et al. (2019).

This project will give valuable understanding into the mechanism of resistance to steroidal drugs in the most common form of breast cancer, which is ER+ BC and are hormone dependent. Investigating the impact of UGT overexpression on drug efficacy may reveal new therapeutic targets. Developing strategies to modulate UGT activity could enhance the existing drug efficacy. The findings from this project might ultimately be translated into clinical use such as development of UGT inhibitors or use of UGT overexpression a biomarker for drug response. This project will also contribute to a more comprehensive understanding of UGT activity in drug resistance, fill the gaps in our knowledge and make clear whether they can be exploited to develop better treatment strategies.

In the light of earlier investigations, the current study aimed to build on the existing foundation by specifically testing the effects of overexpression of UGT2B15 and UGT2B17 in breast cancer cell lines. At the onset of the project, it was planned for both UGT2B15 and UGT2B17 studies to be carried out in parallel. However, it was later decided that studies of UGT2B15 should be prioritized. Thus, all the results shown herein will be derived from experiments using UGT2B15 overexpression models. However, some UGT2B17 overexpression models were also developed during the project, and these will be retained for use in future studies.

The broad research question that will be addressed here is:

Does the overexpression of UGT enzymes affect the anticancer efficacy of steroidal drugs in breast cancer?

To answer this question, we will explore the relationship between UGT overexpression and drug resistance in breast cancer cell lines. The results could have significant implications for current (e.g. tamoxifen) and emerging (e.g. androgen) breast cancer therapies.

1.9 Research Aims and Hypotheses

The following are the hypotheses and aims addressed in this research project:

Hypothesis 1: Transient UGT2B15 overexpression in MCF7 cells will increase the resistance to 4-OH TAM leading to loss of growth inhibition by 4-OH TAM in short term cell growth analysis.

Hypothesis 2: Transient UGT2B15 overexpression in MCF7 cells will reduce the ability of 4-OH TAM to inhibit the estrogen receptor (ER) in short term gene expression analysis.

Hypothesis 3: MCF7 cells with stable UGT2B15 overexpression will outcompete normal MCF7 cells under 4-OH TAM treatment in long term competitive growth assays.

Aim 1: To establish overexpression of transiently transfected UGT2B15 in the ER+ cell line MCF7, and test for 4-OH-TAM sensitivity via cell growth analysis.

Aim 2: To establish overexpression of transiently transfected UGT2B15 in the ER+ cell line MCF7, and test for 4-OH-TAM sensitivity via gene expression analysis.

Aim 3: To establish overexpression of stably transfected UGT2B15 in the ER+ MCF7 cells, and test for 4-OH-TAM sensitivity via fluorescent based competition assay.

By addressing these hypotheses and completing these aims, we seek to get a comprehensive understanding of the role of UGT2B15 in modulating the efficacy of tamoxifen.

2 MATERIALS & METHODS

2.1 Research facilities

The experiments were conducted in the Flinders Health and Medical Research Institute (FHMRI) housed within the College of Medicine and Public Health at Flinders University. All experiments were carried out in Health Medical Research Building (HMRB) physical containment level 2 (PC2) facility.

2.2 Materials

2.2.1 Chemicals & reagents

All chemicals used in this research were of analytical grade. The names of the chemical reagents, along with the names of their respective suppliers, are listed under Appendix 1 Table 6.1.1 The composition of chemical solutions, including cell growth media, are elaborated under Appendix 1 table 6.1.2. Consumables, equipment and software used are included in Appendix 1 table 6.1.3, table 6.1.4, table 6.1.5 respectively.

2.2.2 Breast cancer cell lines

Breast cancer cell lines, MCF-7 and ZR75 were originally supplied by American Type Culture Collection (ATCC) and low passage stocks (< 30 passages) were maintained as frozen stocks within the laboratory. Both lines are derived from human mammary gland epithelial cancer cells and show expression of estrogen receptor (ESR1) and androgen receptor (AR). MCF-7 and ZR75 stable cell lines with overexpression of UGT2B15 and UGT2B17 were already established in the laboratory as part of a previous study and had been maintained as frozen stocks.

2.2.3 Plasmids and expression vectors

Multiple plasmid vectors were used in this study and their maps are provided in Appendix 2. [6.2.1]. These are briefly described below.

1. UGT2B15-pIRES. Expresses a bicistronic cassette that contains the human UGT2B15 gene, an internal ribosome entry site (IRES), and the puromycin acetyltransferase gene. This cassette is under the control of the ubiquitously active human eukaryotic elongation factor 1 alpha (EF1α) promoter. This vector was made within the research group.

2. UGT2B17- pIRES. Expresses a bicistronic cassette that contains the human UGT2B17 gene, an internal ribosome entry site (IRES), and the puromycin acetyltransferase gene. This cassette is under the control of the ubiquitously active human eukaryotic elongation factor 1 alpha (EF1α) promoter. This vector was made within the research group.

3. mCherry-pcDNA3. Expresses the mCherry variant of red fluorescence protein (RFP) under control of the viral CMV promoter. Also expresses a Neomycin resistance gene under control of a viral SV40 promoter. This vector was made within the research group using the pcDNA3 backbone from ThermoFischer (CatLog number V79020).

4. pEYFPN1. Expresses a Yellow variant of enhanced green fluorescence protein (EYFP) under control of the viral CMV promoter. Also expresses a Neomycin resistance gene under control of a viral SV40 promoter. Originally from Clontech. (CatLog number 6006−1).

5. ARR3-Luc. Expresses firefly luciferase under the control of an androgen responsive promoter Generated using the pGL3-promoter vector, pGL3 basic vector and backbone from Promega. (Madison, WI). (CatLog number E1751). Provided by Dr. Theresa Hickey (University of Adelaide).

6. pRL-null. Expresses Renilla luciferase. Originally from Promega (Madison, WI), (CatLog number E2231).

2.2.4 Antibodies

The antibodies used in Western blot were anti-UGT2B15/2B17 which were made previously in this laboratory. A peptide covering the UGT2B15 protein from residues 84 to 167 was used to generate an antibody in rabbits in the antibodies production facilities at South Australian Health and Medical Research Institute (Gilles Plains, Adelaide, Australia). This antibody was previously shown to recognize both UGT2B15 and UGT2B17 but did not cross-react with other UGT2B enzymes as previously reported by Hu, I., et al. (2022).

2.3 Methods

2.3.1 General cell maintenance

Breast cancer cell culture was carried out in a biosafety cabinet using aseptic techniques. The surface and all the equipment before use was sterilised with 80% ethanol. Cells were maintained in growth media which comprised RPMI medium (Gibco) supplemented with 10% FBS and antibiotics and stored in thermoregulatory incubators that was set to maintain CO_2 at 5% and optimal temperature at 37^0C. Detailed composition of the medium is given in Appendix 1. Confluency of the cells in culture plates/flasks were kept under frequent observation by using a microscope. Cells were sub cultured when 80-90% confluent. As and when required the cells were either harvested for various assays as described in sections 2.3.4, 2.3.5, 2.3.6, 2.3.7, and 2.3.8 or transferred to new flask. For each passage, the cells were washed with PBS after removal of the medium using a vacuum aspirator. The PBS was then vacuumed and trypsin solution added at $1/10^{th}$ volume of the original growth media volume. To allow the dissociation of the cells from the surface of the culture plate, the plates were incubated for 5-10 minutes in a 37^0C incubator. Trypsinisation was stopped by the addition of the culture medium (RPMI with 10% FBS). The appropriate volumes added per suitable flasks are included in Table 1 as per guidelines from cell culture protocols by (Thermo Fischer Scientific, 2006a). The cells were either used for further experiments or transferred to a new culture flask. Cells were counted to plate them in different densities depending on the experiment to be performed. Cell counting was performed using a haemocytometer placed under a microscope with 15µL of the cell suspension mounted by a coverslip.

Table 1. Suitable volumes for different cell culture vessels used

Culture vessels used	PBS volume (mL)	Trypsin volume (mL)	Media volume (mL)
T25	4	0.5	4
T75	10	1	10
T125	20	2.3	20
6 well plate	2	0.2	2

Cells were cryopreserved (Thermo Fischer Scientific, 2006b) in liquid nitrogen when needed. Cell suspensions after trypsinisation were recollected into a 10mL tube and centrifuged

at 400g for 5 minutes or until pellets formed. The supernatant was removed, and pellets were then resuspended in 1ml freezing media (FBS with 10% DMSO) and transferred into 1.5mL cryovials. The vials were first stored in -80^{0}C freezer, covered by a cocoon made from paper towel to slow the freezing process. Subsequently, vials were moved to the liquid nitrogen tank for long term storage. To recover the cells from frozen stock, they were quickly thawed by briefly placing the vials in warm beads bath, then transferred into a T25 flask containing fresh growth medium (Thermo Fisher Scientific, 2006).

2.3.2 Lentiviral transductions

For lentivirus production, plasmid DNA mixtures were generated using 3 transfer vectors: GFP-IRES-Puro/pTiger, mCherry -IRES-puro/pTiger, and mCherry2aUGT2B15-IRES-puro/pTiger, together with packaging vectors (Curran et al., 2000). For each viral preparation, 5µL, 2µL and 1.3µL of the transfer plasmids, 3µL gag-pol packaging vector, 3µL VSV-G envelope plasmid and 125 µL serum free DMEM was mixed in one tube marked A while in parallel 22.5µL Lipofectamine and 300 µL serum free media was added in Tube marked B. Both tubes were combined after 5 minutes incubation followed by incubation for 20 minutes at room temperature to allow the complex formation. The transfection mixtures were added to HEK293T cells for viral particle production. 48-72 hours post transfection; viral supernatants were harvested into tubes and centrifuged twice to remove any HEK293T cells. The clarified viral supernatant was combined with polybrene at 1 ug/ml and then used for transducing MCF7 or ZR-75 cells by combining with a cell suspension of 1.5 x 10^6 cells per T25 flask. The MCF-7 and ZR-75 cells were checked for fluorescence every 2 days for the following week to assess transduction efficiency. Four days post-transduction, the cells were selected for puromycin resistance by adding 0.2µg/ml final concentration of puromycin to the media.

2.3.3 Transient transfections in MCF7 cells

MCF7 cells were transfected by the reverse transfection method using Lipofectamine 2000.

To carry out transient transfections of MCF7 cells, transfection mixes were prepared as follows. For each transfection, 1.8µg total DNA containing 0.69µg EYFP, 1.67µg IRES

plasmid or 0.59µg 2B15 plasmid was diluted in 200 µl serum free RPMI to prepare the DNA mixes as A1 or A2 correspondingly. In a separate tube labelled B, 10.8 µl lipofectamine was diluted in 200 µl serum free RPMI. After 5 minutes incubation, B is distributed into A1 and A2 for another incubation at room temperature for 20 minutes to enable complex formation. In parallel, the MCF7 cells were harvested using trypsin and counted using haemocytometer. Using 24 x 10^4 cells suspended in 12.8mL RPMI, cell suspension was prepared and mixed with the pre-prepared transfection mixes. These cell suspension mixes were then aliquoted 150µL per well into 30 wells of the 96 well plate. The plate was then incubated in temperature-controlled incubators for 2 days in order for cell attachment and recovery before media was changed and treatments applied.

To perform transfection for the gene expression analysis using MCF7 cells, the same process was performed as above but the plasmid amounts were optimized for the required cell numbers. For each transfection, 2 mixes of DNA were created, A1 by combining 8µl EYFP, 2.8µl IRES plasmid and 150 µl serum free RPMI. Then A2 contained 9.8µl 2B15 plasmid was diluted in 150µl serum free RPMI. In a separate tube labelled B, 18 µl lipofectamine was diluted in 300µl serum free RPMI. After 5 minutes incubation, B is distributed into A1 and A2 for another incubation at room temperature for 20 minutes to enable complex formation. In parallel, the cells were harvested and counted using haemocytometer. Using 112 x 10^4 cells suspended in 16mL RPMI, cell suspension was prepared and mixed with the pre-prepared transfection mixes. The cell + transfection mixtures were then aliquoted into the wells of a 12 well plate. The plate was then incubated in temperature-controlled incubators for 2 days in order for cell recovery to occur before media was changed and treatments applied.

2.3.4 Culture conditions for cell growth analysis under TAM treatment

X	X	X	X	X	X	X	X	X	X	X	X
X	IRES 1μM	IRES 0.5μM	IRES 0.1μM	IRES 0.05μM	IRES 0μM	2B15 0μM	2B15 0.05μM	2B15 0.1μM	2B15 0.5μM	2B15 1μM	X
X	IRES 1μM	IRES 0.5μM	IRES 0.1μM	IRES 0.05μM	IRES 0μM	2B15 0μM	2B15 0.05μM	2B15 0.1μM	2B15 0.5μM	2B15 1μM	X
X	IRES 1μM	IRES 0.5μM	IRES 0.1μM	IRES 0.05μM	IRES 0μM	2B15 0μM	2B15 0.05μM	2B15 0.1μM	2B15 0.5μM	2B15 1μM	X
X	IRES 1μM	IRES 0.5μM	IRES 0.1μM	IRES 0.05μM	IRES 0μM	2B15 0μM	2B15 0.05μM	2B15 0.1μM	2B15 0.5μM	2B15 1μM	X
X	IRES 1μM	IRES 0.5μM	IRES 0.1μM	IRES 0.05μM	IRES 0μM	2B15 0μM	2B15 0.05μM	2B15 0.1μM	2B15 0.5μM	2B15 1μM	X
X	IRES 1μM	IRES 0.5μM	IRES 0.1μM	IRES 0.05μM	IRES 0μM	2B15 0μM	2B15 0.05μM	2B15 0.1μM	2B15 0.5μM	2B15 1μM	X
X	X	X	X	X	X	X	X	X	X	X	X

Figure 5. **Layout representing a 96 well plate set up for the crystal violet assay using MCF7 cells.**

Wells shown in green colour were seeded with MCF7-IRES transfected cells and those shown in pink are the MCF7-2B15 transfected cells. Each cell type was treated with the indicated doses of TAM [0, 0.05, 0.1, 0.5, 1μM]. Wells marked with X contains no cells. Post drug treatment the cells were checked for viability using crystal violet staining. This setup allows for a sensitive yet rapid method for quantifying MCF7 cells proliferation.

MCF7 cells transiently transfected with either IRES or UGT2B15 plasmids were plated as described above at a cell density of 2 x 10^4 per well which occupied a surface area of $0.32cm^2$. 6 replicate wells were used for each dose condition. This resulted in 60 experimental conditions total distributed across the plate as demonstrated in Figure 5. After 48 hours post plating, cells were checked for density and then rinsed with 1X PBS and the media was replaced with Phenol-red free RPMI with 10% charcoal-stripped FBS (called stripped medium) to which 4-OH TAM had been added at a final concentration of 0, 0.05, 0.1, 0.5, or 1μM. The drug stocks were prepared in ethanol vehicle, and the final concentration of ethanol was 0.1%. After incubating for 5 days, the cells were processed for Crystal violet assay as discussed in 2.3.6.

2.3.5 Culture conditions for gene expression analysis under TAM and E2 treatment

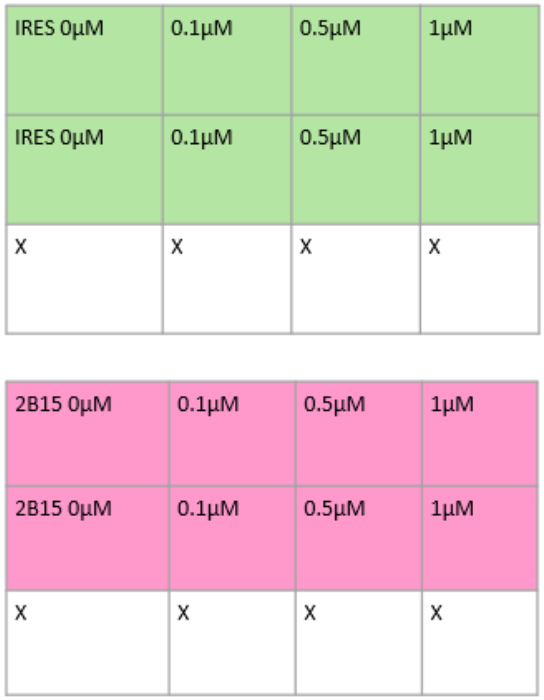

Figure 6. **Layout representing a 12 well plate set up for the gene expression analysis using MCF7 cells**.

Wells in the top plate were seeded with MCF7-IRES transfected cells coloured in green and those in pink in the second plate at the bottom are the MCF7-2B15 transfected cells. Each cell type was treated with the indicated doses of TAM [0,0.1, 0.5, 1µM]. Wells marked with X contains no cells. The cells in the top row in both plates received 1nµM E2 treatment after 5 days while cells in the top row got 0nM E2. This setup allows for the comparison of the gene expression variations among different cell types occurring due to response changes to the drug treatment in the presence or absence of E2.

MCF7 cells transiently transfected with either IRES or UGT2B15 plasmids were plated at a cell density of 14 x 10^4 per well which occupied a surface area of 3.6cm^2. This resulted in 16 experimental conditions in total distributed across 2 plates as demonstrated in Figure 6. After 48 hours post plating, cells were checked for density and then rinsed with 1X PBS and the media was replaced with 2mls of Phenol-red free RPMI with 10% charcoal-stripped FBS

(called stripped medium) to which 4-OH-TAM had been added at a final concentration of 0, 0.1, 0.5, 1µM. After 3 days of culture with 4-OH-TAM, the media was replaced with media containing either 1nM estradiol (E2) or the vehicle (ethanol at 0.1% final concentration). After 2 days E2 treatment, the cells were harvested in TRIzol reagent for preparation of the RNA and qRT-PCR as mentioned in 2.3.7 .

2.3.6 Cell growth analysis

To assay the cellular proliferation, the crystal violet assay was utilised. In a 96 well plate, cells were seeded at a density of 2 x 10^4 cells/well in 150µL RPMI media. After TAM treatment for the duration of 5 days as in section 2.3.4, all the media was vacuum aspiration and 50 µL of the crystal violet stain was added (see Appendix 1). After incubation at room temperature to allow staining of the cells for 20 mins, the stain was removed taking care not to disturb the cells. The plate was washed with water thrice, each time dipping the plate in a tray full of water and allowing the stain to lift from the wells and be cleared until no excess stain was remaining. These plates were drying in the fume hood with the fan ON for 20 mins. 100 µL of 30% acetic acid was added for solubilizing the fixed and stained cells and the plates put on shaker to enhance solubilisation for around 20 mins. Then the optical density of the plates was measured in iD5 plate reader with absorbance read at 636nm. The data exported to excel for further analysis, including determining the average and standard deviation of the replicates for each condition, and normalizing the values for each treatment over the values of the vehicle control.

2.3.7 Gene expression analysis

Cells grown in 12 well plates were harvested 48 hours after transfection for RNA analysis (Cai et al., 2023). Comparative abundance of the target mRNA, pS2 (also known as trefoil factor 1, TFF1) (Brown et al., 1984) was calculated relative to the housekeeping gene, glyceraldehyde 3-phosphate dehydrogenase (GAPDH). Primers sequences are listed in Appendix 2 [6.2.2].

2.3.7.1 RNA Extraction

RNA was extracted from the cells cultured in 12 well plates using TRIzol (Invitrogen) followed by DNase treatment and reverse transcription using NextGen MuLV transcriptase (Lucigen) as per the manufacturers protocol. Firstly, the cells were harvested with 0.5mL TRIzol reagent by keeping the plates in -20^{o}C freezer overnight. The contents from each of the wells were then transferred to labelled microcentrifuge tubes and 100µL chloroform was added. The tubes were mixed thoroughly, vortexed until it turned milky pink and centrifuged at 12,000rpm for 15 minutes. Meanwhile new tubes were labelled and placed in rack which received 350 µL 100 isopropanol and 0.5 µL 10mg/ml glycogen. The aqueous layer from each tube was transferred into the Eppendorf tube containing the isopropanol/glycogen and the tubes were incubated at -20^{o}C for 10 minutes and centrifuged at 12,000rpm. RNA pellets were washed with 1ml of 80% ethanol and centrifuged as above, the supernatant was removed and the pellets air dried by placing them overnight on the bench top. Ensuring that the ethanol has vaporised completely, the pellets were redissolved in 40µL nuclease free water followed by heating at 70^{0}C on a heat block to aid dissolution. RNA was quantified using a Nanodrop.

2.3.7.2 cDNA Synthesis

The process of cDNA synthesis involved 2 steps – DNase reaction followed by a Reverse transcription (RT). DNase treatment was applied to all RNA samples before RT to remove residual genomic DNA if present. The required volume to provide the desired amount of RNA was calculated from the RNA concentration measured using the nanodrop. This known quantity of RNA was combined with the DNase treatment reaction mix as shown in Table 2.

Table 2. DNase treatment mix for a single reaction

Reagents added	**Volume Per tube (µL)**
10x Buffer	2.0
RNase inhibitor	0.4
DNase	0.4
RNA	tbd
Nuclease free water	tbd

For 16 samples, a 18x DNase master mix was prepared with the above calculations and distributed equally in all tubes and the RNA added. This 20µL reaction mix was incubated at 25-37^{0}C for 10 minutes. Inactivation of the DNase was done by the addition of 1µL 25mM EDTA followed by incubation for 10 minutes at 75^{0}C.

For reverse transcription (RT), half of each DNase reaction mix was transferred to a new tube with the required RT reaction mix as shown in table 3.

Table 3. RT reaction mix for a single tube

Reagents added	**Volume Per tube (µL)**
dNTPs 10mM	1.5
Random primers 50ug/ml	1.5
RT Buffer	4.1
Nuclease free water	13.2
RNase inhibitor	0.4
Reverse transcriptase	0.4
DNase reaction	20.0

For 16 samples a 18x RT master mix was made and aliquoted equal volume into each tube. This reaction mix was incubated for 5-10 minutes at 25^{0}C then at 42^{0}C for 60-90 minutes and an optional step of 70^{0}C incubation for 10 minutes to inactivate. Following cDNA synthesis, all the tubes containing cDNA samples were diluted 2-fold with nuclease free water and stored at -20^{0}C until qPCR was performed.

2.3.7.3 qRT-PCR

qRT-PCR was performed to quantify mRNA levels of the transiently transfected control and overexpression MCF7 cells (Wang et al., 2024). Estrogen regulated PS2 was analysed together with the 18s and GAP-DH housekeeping genes. The sequences of the primers used in this study is provided in Appendix 2. Duplicate reactions were performed for each sample in qPCR (e.g. 32 reactions each primer for 16 samples).

Table 4.Promega Go Taq qRT-PCR mix per tube

Reagent added	**Volume per tube (µL)**
Go Taq master mix	8.0
5mM primer F+R mixture	2.0
PCR clean water	4.0

For 16 samples, a 34x master mix was made for each primer pair (as shown in table 4) which was sufficient for duplicate reactions plus residual volume for carrying out a negative template control (NTC). 14µL of the master mix was aliquoted into 33 tubes (32 samples + NTC). 2µL of diluted cDNA prepared in section 2.3.10 was pipetted into each of the PCR tube except the NTC. The PCR tubes were then capped and cycled in a Rotor Gene Q using the protocol established previously in the laboratory. qPCR cycling conditions were as shown in Table 5. qRT-PCR Cycling conditions under different steps of the process. Analysis of the results after PCR run was conducted using the Rotor Gene Q software 2.3.4 with a threshold set at 0.08. The cycle number at which the threshold was crossed (Orrantia-Borunda et al., 2022) for each reaction was determined and this was exported as an excel analysis data sheet and further calculations were performed in excel. Briefly, this involved using the delta Ct method to determine the difference in the Ct values for the target gene (e.g. PS2) and the housekeeping gene (e.g. GAP-DH) using the equation: delta Ct = Ct (target gene) – Ct (housekeeping gene). To determine the relative expression the following equation was used: Relative expression = 2^deltaCt, which assumes an amplification efficiency of 2 for the primer pair. The fold change in expression of the target gene was then calculated by comparing the treatment conditions to the vehicle conditions. This involved first normalizing expression in the E2 treated samples to their respective vehicle treated control samples for each 4-OH-TAM treatment condition; then secondarily, comparing each of the 4-OH-TAM treated conditions to the vehicle control.

Table 5. qRT-PCR Cycling conditions under different steps of the process

qPCR cycling conditions	**Temperature (^{0}C)**	**Duration**
Initial activation	95	5 minutes
Cycling (35 cycles) Denaturation Annealing	 95 60	 15 seconds 10 seconds
Melting	95	90 seconds

2.3.8 Statistical analysis

All statistics were analysed using Microsoft Excel and R Studio program. Significance of the differences between treatment conditions was determined using one way ANOVA with Tukey Post-Hoc tests where applicable. Statistical significance is indicated as $p<0.05$ *, $p<0.01$ **, $p<0.005$ ***. The analysis was conducted using the R Studio packages with the functions Avo and Tukey HSD. Input code and the detailed statistical analysis output from R studio are shown in Appendix 3 [6.3.2]. Statistics were not applied to the data without sufficient independent experiments or satisfactory number of replicates.

2.3.9 Luciferase assay

To carry out Luciferase assay, forward transfection [Appendix 3] was conducted in a 96 well plates containing cells that had been previous cultured with different doses of 4-OH-TAM for 5 days. Two plasmids were combined 1µg of ERE-TK-Luc (Firefly) and 0.1µg of pRLNull (Renilla) plasmids combined in a tube with 60µL SF RPMI. A second tube was prepared with 2.7µL lipofectamine combined with 60µL SF RPMI. After a 5-minute incubation, both tubes contents were combined and incubated 20 minutes. The mixture was then diluted with 560ml SF RPMI providing enough volume to add 10µL into each of 68 wells. Cells were solubilised 48 hours post forward transfection by the addition of 100µL Passive Lysis Buffer (PLB) per well. A gentle yet constant shaking of the plates for 15 minutes to produce complete lysis. A 20µL sample of lysate was used for analysis on the Top Count Luminescence and Scintillation counter (Packard, Australia) with the dual-luciferase reporter assay system (Promega) that measures both firefly (*Phontinus pyralis*) and Renilla Luciferase activity. To minimise the effect of luminescence carryover from adjacent wells, cell lysates

were loaded onto non-adjacent wells in a 96 well plate. The lysates were mixed with 30µL firefly luciferase agent to assess the luciferase activity generated from the transiently transfected ERE-TK-Luc vector. Luminescence was read within 2 minutes. Then 50µL Stop-and-Glo reagent was added to each of the wells to stop the firefly activity and provide the substrate for Renilla enzyme made by the pRLNull vector. Again, the luminescence was read within 2 minutes following substrate addition. Relative activities were calculated as the ratio of firefly/Renilla activity.

2.3.10 SDS-PAGE and Western blot

Western blot analysis was used for analysis of UGT-expressing stable cell lines that had been previously generated in this laboratory and were recovered from cryopreservation and modified for long-term competition assays as described in section 2.3-11. Stable cell lines cultured in 6 well plates were scraped using a new scraper in 1ml sterile PBS after removal of the media. The cell suspension was transferred to 1.5ml Eppendorf tubes. The cell pellets were collected by centrifugation at 5000 rpm for 10 minutes. The pellets were resuspended in a hypotonic buffer 10mMTris 1mM EDTA pH 7.6 (TE) buffer (Appendix 1) and subjected to3 cycles of freezing and thawing by keeping the Eppendorf tubes in -80 freezer for 20 minutes and then taking them outside to the benchtop to place them in room temperature for 20 minutes and repeating these for 3 times. This allows gentle lysis and preserves enzyme integrity in case enzymatic activity assays are required. Estimation of protein concentration was performed by selecting the A280 proteins setting the 340nm for correction. Aliquots of 25µg for each lysate were combined with SDS-PAGE loading dye (Appendix 1) at 1 x final concentration and heated to 80^{o}C for 10 min. The samples were separated by SDS-Polyacrylamide gel electrophoresis (SDS-PAGE) by first running the samples at 60v for 30 minutes through the stacking gel and then 120v for 60-90 minutes through the separating gel or until when the tracking gel reaches the bottom in a Mini Protean ll Cell instrument (Laboratories). The gel containing the separated proteins were blotted onto nitrocellulose membrane using Tris-Glycine buffer with 15% methanol (Appendix 1) using low voltage (15v) overnight at 4^{o}C. The membranes were stained with Ponceau solution (0.1% Ponceau red in 5% acetic acid) and then rinsed in water and imaged for estimation of protein loading. Next, the membranes were blocked in 3% non-fat milk powder in Tris-buffered saline with 0.1% Tween-20 (TBST) (Appendix 1) followed by probing with primary antibody 1:2000 dilutions in 1% NFM in TBST overnight at 4^{0}C. After

TBST washing thrice for 10 minutes each time, the membrane was incubated with horseradish peroxidase conjugated donkey anti-rabbit antibody (Neo Markers). 1:5000 dilution in TBST for 2 hours at room temperature. Immunosignals were revealed using Super Signal® West Pico Chemiluminescent substrate (Thermo-Scientific) in a Chemidoc (Laboratories). In some experiments, membranes were re-probed with an anti-actin antibody for normalisation (Sigma-Aldrich).

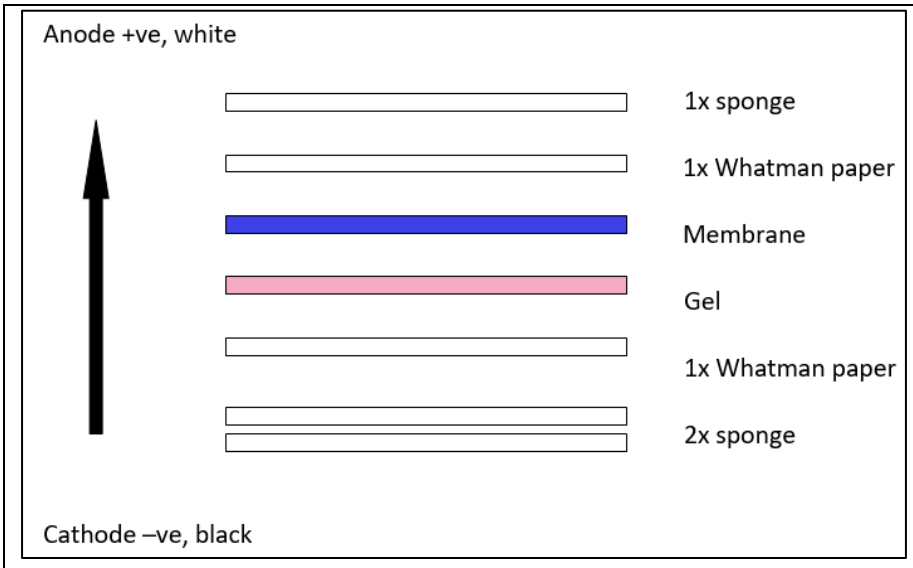

Figure 7. **Setting up of gel membrane sandwich for use in Bio-Rad Apparatus (Laboratories)**

2.3.11 Generation of stable fluorescently labelled MCF7 cells for competition assay

To study the competitive growth between the stably transfected MCF7 cells, a fluorescence-based competition assay was devised. For this assay, the pIRES and UGT2B15-pIRES MCF7 stable cell lines that had been previously generated in the laboratory and validated for expression by immunoblotting (section 2.3.10) were stably transfected with either the mCherry or pEYFP-N1 vector.

The plasmid transfection protocol was performed using Lipofectamine 2000 as follows: 2µg of mCherry-pcDNA3 or pEYFPN1 plasmids were placed into separate tubes with 100µL serum media. Separately 10 µL lipofectamine was combined with the 200µL serum free media. After 5 minutes incubation 100µl of the Lipofectamine solution was added to each of the

plasmid solutions and incubated 20 minutes. Each of these complexes were then added to a separate flask containing of the MCF7 stable cell lines, i.e. the pIRES-MCF7 cell line was transfected with the mCherry-pcDNA3 plasmid and the UGT2B15-pIRES-MCF7 cell line was transfected with the pEYFPN1 plasmid.

Three-days post-transfection, the cultures were treated with 400µg/mL G418 in fresh culture media. Over the subsequent 3 weeks, media was changed regularly to remove dead cells. Once G418-resistant colonies were visible under the microscope and no further cell death occurred, the cells were examined by fluorescence microscopy using the EVOS. Some colonies that did not show fluorescence were removed by scraping them with a pipette tip (under the microscope) and then rinsing the flask to remove the detached cells. Subsequently, the remaining attached colonies within each flask were detached from the plate using trypsin, pooled, and replated to create a population of fluorescently labelled cells with varying integration sites. The entire transfection and G418 selection process was performed twice, resulting in generation of two independent populations for each of the double-stable cell lines. These are referred to as IRES-mCherry line 1, IRES-mCherry line 2, UGT2B15-EYFP line 1 and UGT2B15-EYFP line 2. Each line is resistant to both puromycin (due to the previously integrated pIRES or UGT2B15-pIRES vector), and G418 (due to the newly integrated pEYFP-N1 or mCherry-pcDNA3 vector). The lines were therefore maintained in RPMI media with both 0.2ug/ml puromycin and 400µg/ml G418.

2.3.12 Competition assay using fluorescently labelled MCF7 cells with UGT2B15 gene overexpressed

Cells were counted prior to the assay. Equal number of MCF7-IRES-mCherry and MCF7-UGT2B15-EYFP were combined into wells in a 6 well plate with RPMI media (El Debs et al., 2011). 48 hours post seeding, the cells were checked for attachment and media was replaced with steroid-depleted RPMI containing varying doses of 4-OH-TAM (0, 0.05, 0.1, 0.5, and 1µM). The plates were incubated for 1 week and then cells were removed from the plates with trypsin and replated in complete RPMI. After allowing 48 hours for cells to attach and recover, the media was replaced with steroid-depleted RPMI containing varying doses of 4-OH-TAM (0, 0.05, 0.1, 0.5, and 1µM). The plates were incubated for another 1 week and then images were captured at 2X magnification using the EVOS-FL with red and green filter sets. Fluorescent cell quantification used the ImageJ platform. TIFF files were imported, and a signal

threshold was set after selecting ‘dark background’. Cell counting was performed using the Analyse Particles module. To filter out debris or artifacts, the size threshold was set between approximately 30 – 350µm² (to accommodate condensed cells and cell clusters), and circularity was set at 0.1–1.0. The exported data was the number of defined regions of interest (ROI), the total area (ROI combined), the average ROI size and % area within the defined ROI. 6-8 panels were imaged for each condition and the results averaged. Because only a single pilot experiment was performed, no statistical analysis was performed.

2.3.13 Compliance to ethics

This project did not involve human or animals subjects. The project had approval from the Flinders Institutional Biosafety Committee (IBC) for exempt dealings with human cells lines (#2011-05). No risk category organism was involved in this study. All experiments were performed wearing personal protective equipment (PPE) in a certified PC2 laboratory using appropriate handling techniques to protect fellow researchers and environment. Risk assessments were completed prior to start of experimental procedures and relevant biosafety and chemical handling trainings attended.

2.3.14 Illustration of overall experimental design

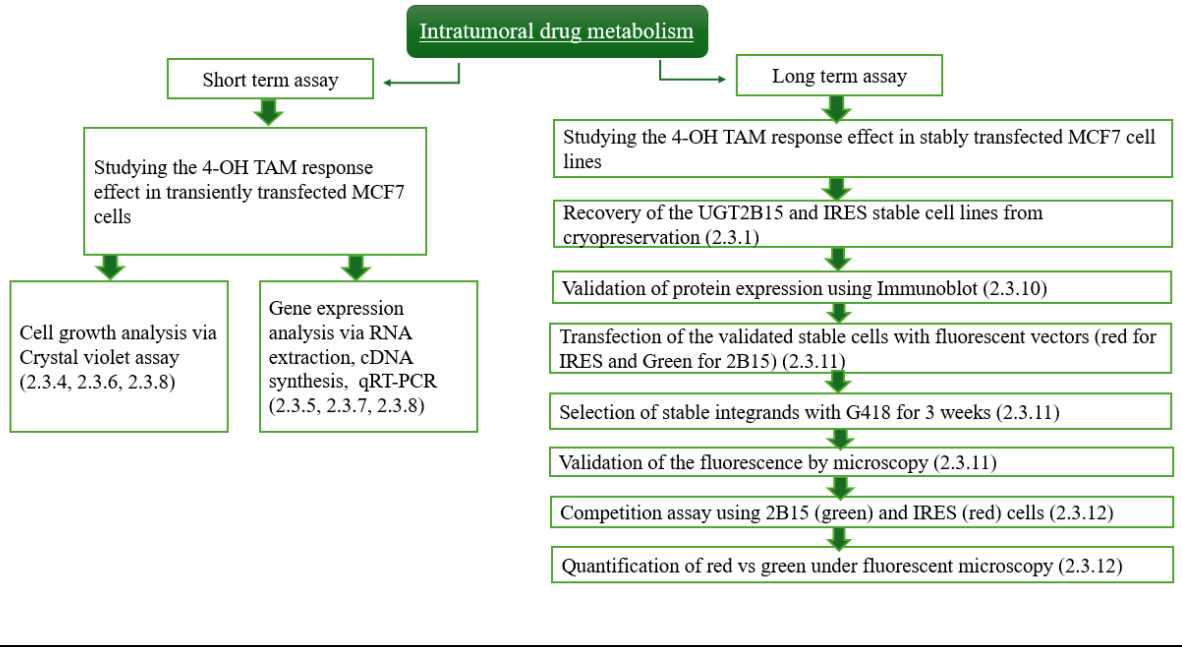

Figure 8. **Flowchart illustrating the overall experimental design of the current study**.

3 RESULTS

3.1 Analysis of Proliferation response to 4-OH-TAM in MCF7 cells transiently transfected with UGT2B15

Pilot studies were performed to establish optimal conditions for study of 4-OH-TAM sensitivity in MCF7 cells. These studies used cells transiently transfected with the empty vector pIRES and cells transfected with the UGT2B15-pIRES vector. These transfected MCF7 cells were plated in 96 well plates and treated with increasing doses of the drug (0, 0.05, 0.1, 0.5, 1µM) in steroid-depleted media for 5 days and then cell density was measured using the crystal violet assay (CVA) as in the Methods section 2.3.6. A dose dependent inhibition of cell growth was observed under these conditions with maximal inhibition at 1uM 4-OH-TAM. The pilot studies also indicated that cells transiently transfected with UGT2B15 showed less inhibition of growth than cells transiently transfected with the empty IRES control plasmid at the three lower doses (0.05, 0.1 and 0.5uM), but not at the highest dose (1uM) (Figure 10). Overall, these data suggest that the conditions established in the pilot study were suitable to analyse the dose dependent effect of 4-OHTAM on MCF7 cells, and also to distinguish a possible protective effect of UGT2B15 expression. These conditions were therefore applied for the further studies.

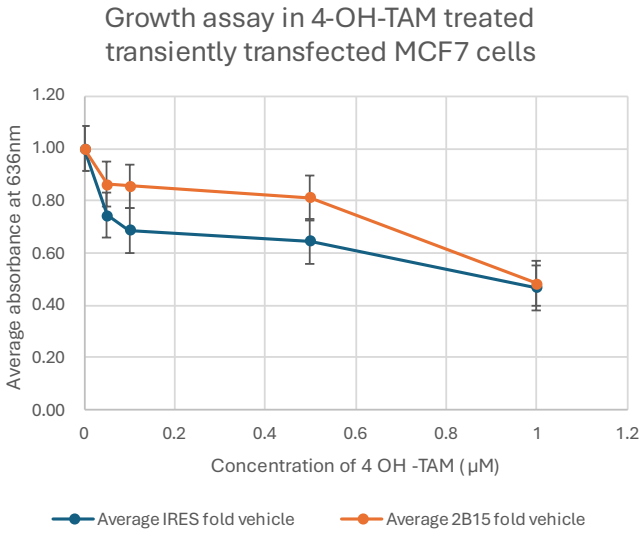

Figure 9. **Cell viability of transiently transfected MCF7 cells measuring growth response at varying concentrations of 4-OH TAM (0, 0.05, 0.1, 0.5, 1µM) for the duration of 5 days in a steroid deplete media**.

Transiently transfected cells were plated at density of 0.3 x 10^4 cells per well in a 96 well plate with 68 well replicates, 2 days prior to drug treatment. The plates were read using iD5 plate reader at an absorbance of 636nm via crystal violet method. The cells were stained with crystal violet stain, washed and solubilised with 30% acetic acid. The concentrations of TAM are given in 1nM along the x axis and mean absorbance is given along the y axis. The graph was generated from a two biological replicates with 60 technical replicates each with the help of excel analysis workbook sheet; statistical analyses were not performed.

Four independent biological replicates of the 4-OH-TAM growth response assay were set up in MCF7 cells using the same transient transfection and drug treatment conditions used in the pilot study (see Figure 10). The results of each experiment were averaged, and the statistical significance of the differences was analysed using ANOVA followed by a Tukey HSD post-hoc test as in the Methods section. The data is presented in Figure 10 with the between-group comparisons shown on two different versions of the bar chart for clarity. In panel A, the cell density after treatment with each drug dose is compared to the cell density in the vehicle condition (0μM), within each transfection condition. In the IRES-transfected condition, cell density was significantly reduced at every dose of 4-OH-TAM as when compared to the vehicle ($p < 0.05$). In contrast, in the UGT2B15-transfected condition, cell density was only significantly reduced at the highest dose of 4-OH-TAM as compared to the vehicle ($p < 0.01$). This suggests that UGT2B15 expression protects cells from the inhibitory effects of 4-OH-TAM at 0.05, 0.1, and 0.5μM doses, but not at the 1μM dose. In panel B, the cell density is compared between the IRES-transfected and UGT2B15-transfected populations at each treatment dose. The difference between the relative cell density was only significant at 0.05μM 4-OH-TAM ($p < 0.05$). This suggests that the UGT2B15 expression protects cells from the inhibitory effects of 4-OH-TAM, but only at the lowest dose used in the study.

Collectively these data are supportive of the hypothesis that overexpression of UGT2B15 confers resistance to 4-OH-TAM; however, the effect may not be significant at doses greater than 0.05μM. The differences between the outcomes of the statistical analyses (panel A vs B) may be due to the high variance between the four replicates.

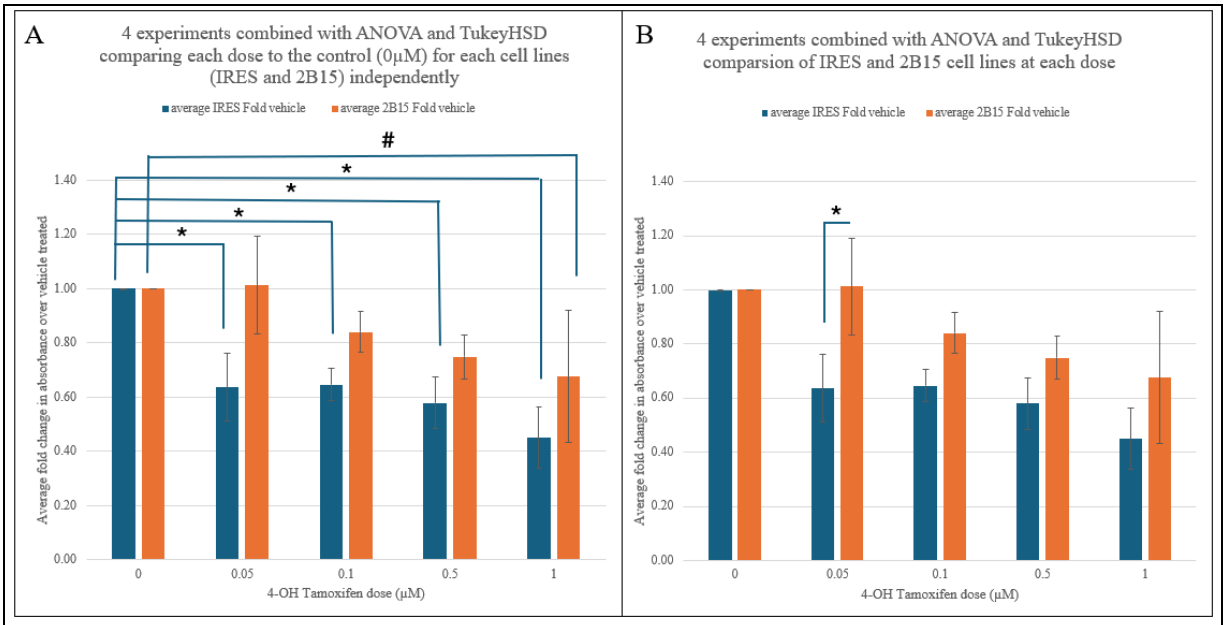

Figure 10. **Statistical study comparing mean absorbance of IRES and 2B15 cell lines at each dose, collected from transiently transfected IRES and 2B15 cell lines obtained from 4 independent experiments**.

The y axis shows the average fold change in cell absorbance (relative to vehicle treatment) and the x axis shows the drug dose. Data is shown as mean and standard deviation. Average absorbance are shown for MCF7 cells expressing the control vector (as blue bars) and the overexpressing UGT2B15 plasmid (as orange bars) after TAM treatment for 5 days with increasing doses. Data combined in this graph are from 5 biologic experiments including normalisation to the vehicle control for every cell line. ANOVA was used to perfom statistical analysis with Tukey HSD post hoc test at $p<0.05$ for the difference between IRES and UGT2B15 at dose 0.05 μM indicated by *. Error bars are created representing standard deviation.

3.2 Confirmation of UGT2B15 overexpression

To confirm over-expression of UGT2B15 in the transiently transfected cells used in these studies, cells that were transfected and maintained in culture for 7 days as in section 3.1. were collected for preparation of RNA and cDNA. The UGT2B15 cDNA was then amplified by qRT-PCR. The bar graph in Figure 11 illustrates the expression of UGT2B15 in UGT2B15-transfected cells and IRES-transfected control cells across 3 independent experiments. The

expression value is shown in arbitrary units normalized to GAPDH expression using the 2^-delta Ct method (Rao et al., 2013) (Livak & Schmittgen, 2001). All transfection experiments showed much higher expression of UGT2B15 in the UGT2B15-transfected cells (450, 108, 211 units respectively) relative to the IRES-transfected cells. However, the level of endogenous UGT2B15 expression in the IRES-transfected control cells was much higher in experiments 2 and 3 relative to experiment 1. These data confirm that the transfection conditions produced high level expression of UGT2B15 that was sustained for at least 7 days post-transfection. It also indicates that the basal UGT2B15 expression may have varied between experiments which may have affected the variability of the responses.

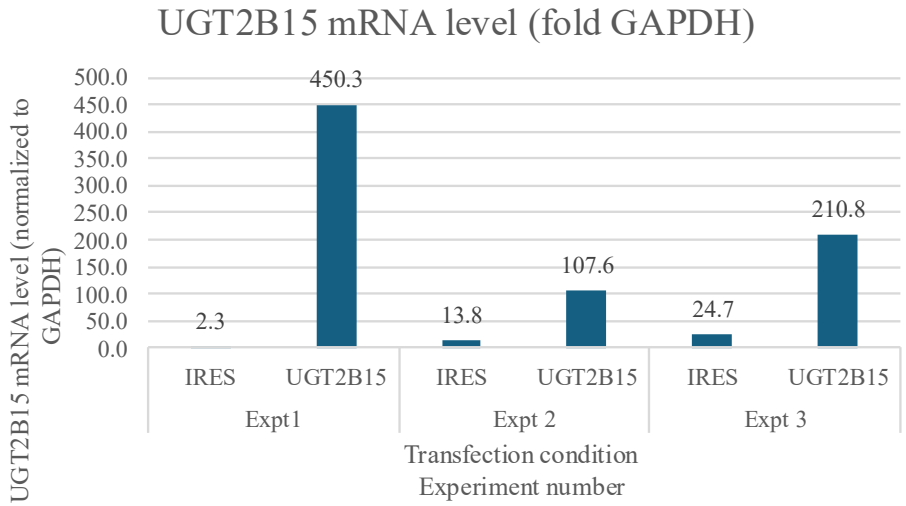

Figure 11. **Overexpression of UGT2B15 gene in transfected MCF7 cells between 4 independent experiments**.

Bar graph of UGT2B15 mRNA expression in MCF7 cells transfected with either the UGT2B15 plasmid or the control vector (IRES), quantified by qRT-PCR. UGT2B15 expression is normalized to GAPDH expression in each sample. Results shown are from 3 independent experiments. These results confirm effective overexpression of UGT2B15 in the UGT2B15 transfected population of MCF7 cells in comparison to the IRES transfected cells (control condition).

3.3 Analysis of estrogen induced gene expression response after 4-OH-TAM treatment in MCF7 cells transiently transfected with UGT2B15 expression plasmids or control plasmids

4-OH-TAM competitively inhibits the binding of estradiol (E2) to the ER, which prevents ERα from activating its target genes. In this sub aim, the transcriptional activation of a classical ERα target gene, PS2, was used as an indicator of 4-OH-TAM effect in MCF7 cells. Cells that had been transiently transfected with either the empty IRES vector or the UGT2B15 vector were pre-treated varying doses of 4-OH-TAM (0, 0.1, 0.5 and 1μM) for 5 days. They were then treated with E2 (1nM) for 48 hrs to induce PS2 expression. RNA was then prepared and used for qRT-PCR analysis of PS2 mRNA level. Figure 12 shows PS2 induction by E2 in cells treated with three doses of 4-OH-TAM (0.1, 0.5 and 1μM) as fold change relative to the non-4-OH-TAM treated condition (0μM). The data shown is the average of three biological replicates.

In the empty vector (IRES) transfected condition, induction of PS2 expression by E2 appeared to be reduced by 0.5μM and 1μM 4-OH-TAM, but the effect was not statistically significant. In addition, the amount of inhibition was not dose dependent (i.e. it did not change linearly with dose). In the UGT2B15 transfected condition, induction of PS2 expression by E2 appeared to be reduced by 0.5μM and 1μM 4-OH-TAM, and the effect was greatest at the highest dose; however, again the changes were not statistically significant. The results of ANOVA and Tukey post hoc test are shown in Appendix 3. The model found that, while that dose was a significant factor, there was no significant difference between any pair of conditions which was likely due to high variability. Overall, the data does not support the idea that UGT2B15 can affect the ability of 4-OH-TAM to inhibit the induction of ERα by E2; however, it is difficult to draw clear conclusions because 4-OH-TAM did not significantly reduce ERα induction in the empty vector (IRES) transfection condition.

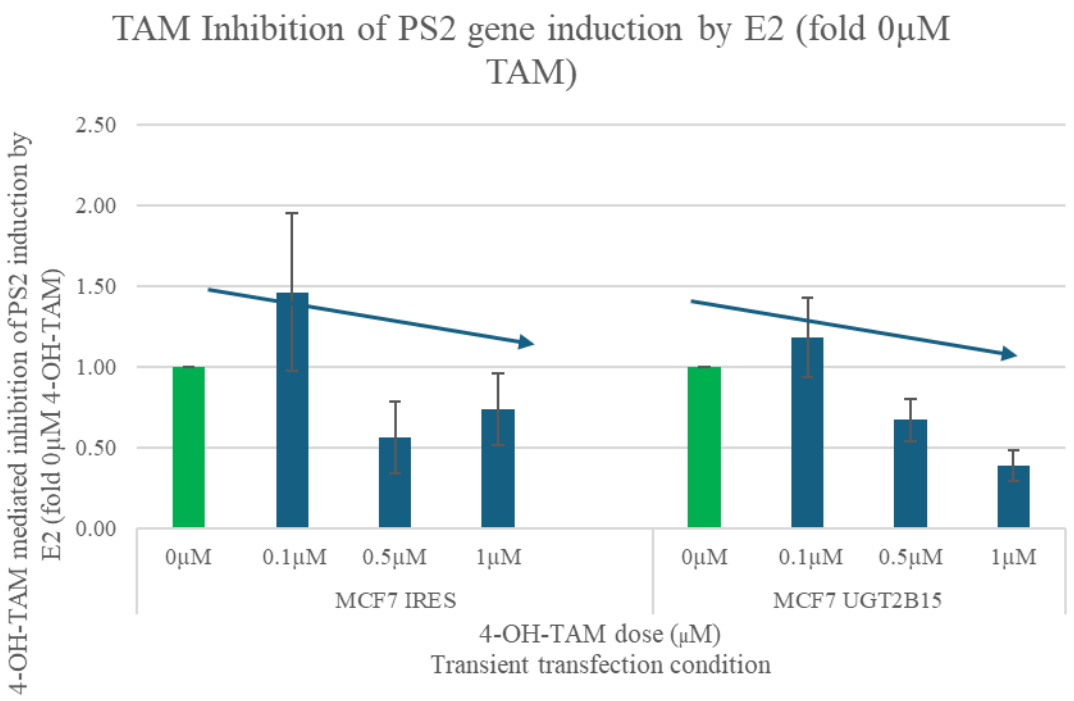

Figure 12. **Inhibition of E2-mediated PS2 gene induction by pretreatment with different doses of 4-OH-TAM in transiently transfected MCF7 cells**.

Bar graph depicting fold induction of PS2 gene expression by E2 in cells treated with 0.1, 0.5 or 1uM 4-OH-TAM, normalized to the non-4OH-TAM treated control condition. Data is the average and standard deviation are from 4 biologic experiments. The arrows emphasize that there is a trend towards reduced PS2 induction with higher doses of 4-OH-TAM; however, ANOVA and Tukey HSD showed no significant difference between any pair of conditions.

3.4 Confirmation of UGT2B15 expression in previously established MCF7 stable cell lines by Immunoblotting

To study the effects of UGT2B15 on long-term 4-OH-TAM response, a competition assay was devised that involves co-culturing cells with low and high UGT2B15 expression in the presence of 4-OH-TAM over multiple cell passages. Because this assay requires long term culture, it requires stably transfected cell line models. Initially, we attempted to generate these cell models using lentiviral vectors that express both the UGT gene and a fluorescent protein marker gene. However, due to technical issues, this approach was not successful. Therefore, an alternative approach was devised that used stable MCF7 cell lines that were previously

developed by a former PhD student in the laboratory. The cell lines had stable integration of either the empty IRES vector or the UGT2B15-pIRES vector. To confirm the latter was still overexpressing the UGT2B15 protein after recovery from cryostorage, immunoblotting was performed.

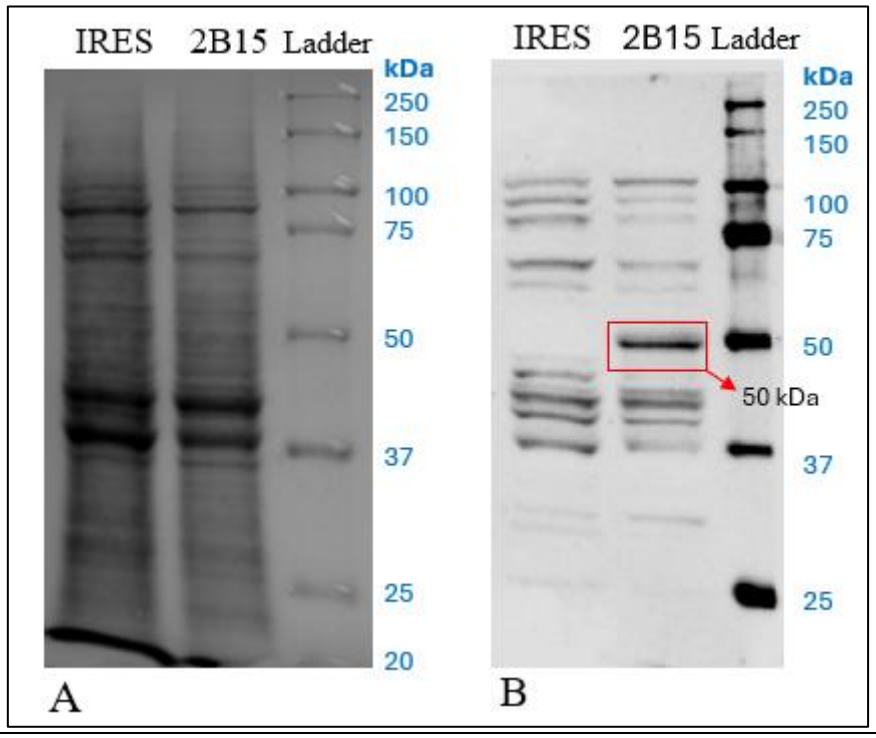

Figure 13. **Analysis of UGT2B15 protein expression in MCF7 stable cell lines by using Immunoblotting**.

(A) Image depicting protein from MCF7 -IRES and MCF7-2B15 stable cell lines separated in SDS-PAGE and stained with Ponceau red.(B) Immunoblot image of the same samples probes with anti-UGT2B15/17. A band of the expected size of UGT2B15 protein (~50kDa, marked by a red box and arrow) appears in MCF7-2B15 cell line and not in MCF7-IRES, confirming the expression of the UGT2B15 construct in the cell line. Protein size standards are shown at the right end of the gel images with the sizes (in kDa) marked in blue for size reference.

Figure 13 shows the result of immunoblotting analysis of total protein prepared from the MCF7-IRES and MCF7-UGT2B15 stable cell lines according to the methods sections. Panel A shows the proteins stained with Ponceau S to estimate loading. The proteins were well resolved and without any observable degradation; however, the protein loading is not identical with slightly more total protein apparent in the IRES sample. Panel B shows the proteins immunoblotted using an anti-UGT2B15/17 antibody, illustrating a distinct signal at ~50kDa in

the MCF-UGT2B15 sample, which is the expected size of the protein. The band did not appear in the MCF-IRES control cell line. These results validate the overexpression of UGT2B15 in MCF7 cells, allowing their application in the subsequent development of the competition assay.

3.5 Generation of fluorescently labelled "double-stable" populations of MCF7 cells expressing UGT2B15, or control vectors and its confirmation of expression by Fluorescence microscopy

The next step of developing the competition assay was to label the UGT2B15-overexpressing and control cells with different fluorescent proteins so that they could be distinguished in co-culture. The MCF7-IRES control stable cell line was transfected with the mCherry-pcDNA3 vector that expresses a red fluorescent protein, while the MCF7-UGT2B15 stable cell line was transfected with the pEYFPN1 vector that expresses the yellow-shifted variant of the enhanced green fluorescent protein. Cell populations with stable integration of these plasmids were generated by selection with G418 as described in the Methods section 2.3.11.

Fluorescence microscopy was used to confirm the efficient production of the fluorescent proteins in the double stable MCF-7 cell lines, designated MCF7-UGT2B15-EYFP and MCF7-IRES-mCherry. Figure 14 shows strong green or red fluorescence in at least 70% of the cells for each of the two cell lines, confirming their suitability for use in the subsequent development of the competition assay.

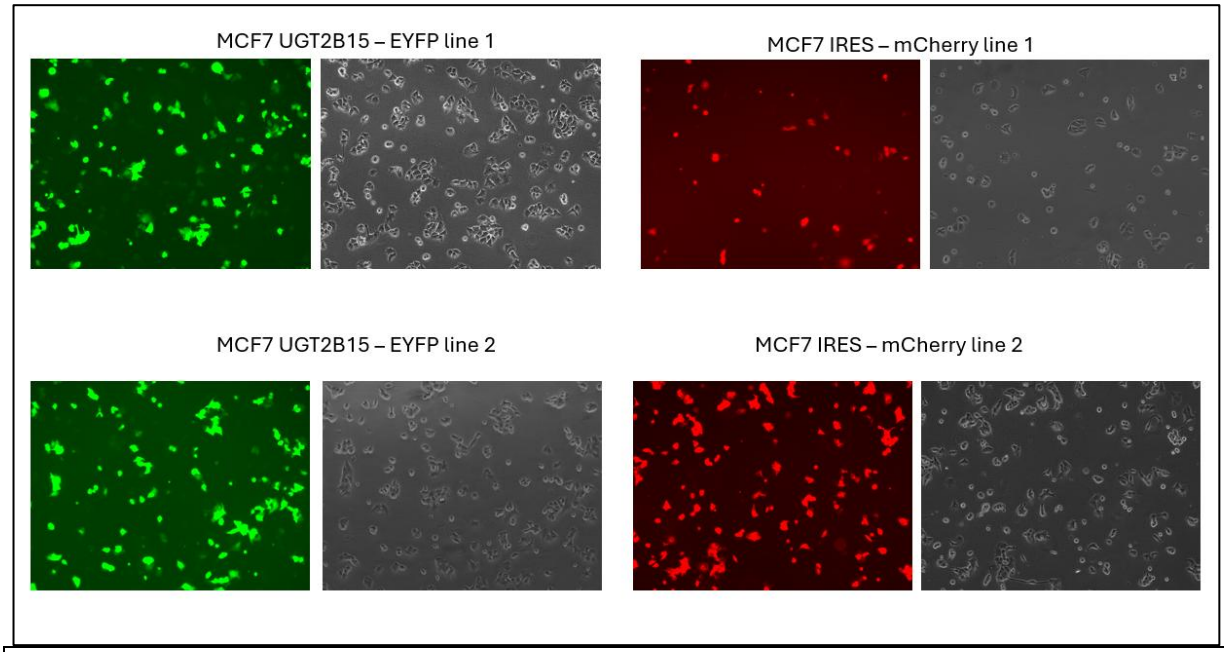

Figure 14. **Confirmation of double stable MCF7cells expressing either green or red fluorescent proteins**.

Fluorescence microscope images of MCF7 breast cancer cell lines that are double stable are presented along with their corresponding images under white light. Representative images are from 2 sets of transfections-with first set presented on top and the second at the bottom. The MCF-7 cells expressing UGT2B15 and EYFP shows green fluorescence (on left panel) while the MCF-7s expressing IRES and mCherry shows red fluorescence (on right panel).

3.6 Analysis of pilot competition assay using double-stable UGT2B15 and control cell lines via fluorescence microscopy

A pilot competition assay was performed as described in the Methods. Briefly, MCF7-UGT2B15-EYFP and MCF7-IRES-mCherry cells were combined in equal numbers, plated in multiple culture wells, and treated with varying doses of 4-OH-TAM (0, 0.05, 0.1, 0.5 and 1µM). Cells were cultured for 1 week and then trypsinized and re-seeded into new wells and cultured for another week with various doses of 4-OH-TAM. The cells were then imaged by

fluorescence microscopy. Figure 14 shows representative images of the co-cultured cells under each of the 4-OH-TAM treatment conditions. It was observed that the untreated cells had become fully confluent by one week; however, the drug treated cells showed a dose dependent slowing of growth and remained sub-confluent.

Cells were quantified in multiple cell fields (images) for each condition using Image J as described in the Methods 2.3.12 and the results are shown in Figure 15. Given that this was only a pilot study, no statistical analysis was performed. The number of UGT2B15-EYFP (green) and MCF7-IRES-mCherry (red) cells were quantified and presented as a ratio (green: red, panel B). This showed that there were more green than red cells under all conditions including the vehicle treatment (0μM 4-OH-TAM). This may have been due to inconsistent plating. There appeared to be a trend towards a higher ratio of green: red cells at doses of 4-OH-TAM > 0.1μM; however, there was high variability between the individual cell fields that were counted, and no statistical analysis was performed. The number of total cells were also estimated using measurements of total area of fluorescence (Figure 15 panel C). These indicated that the number of cells were dose-dependently reduced by 4-OH-TAM.

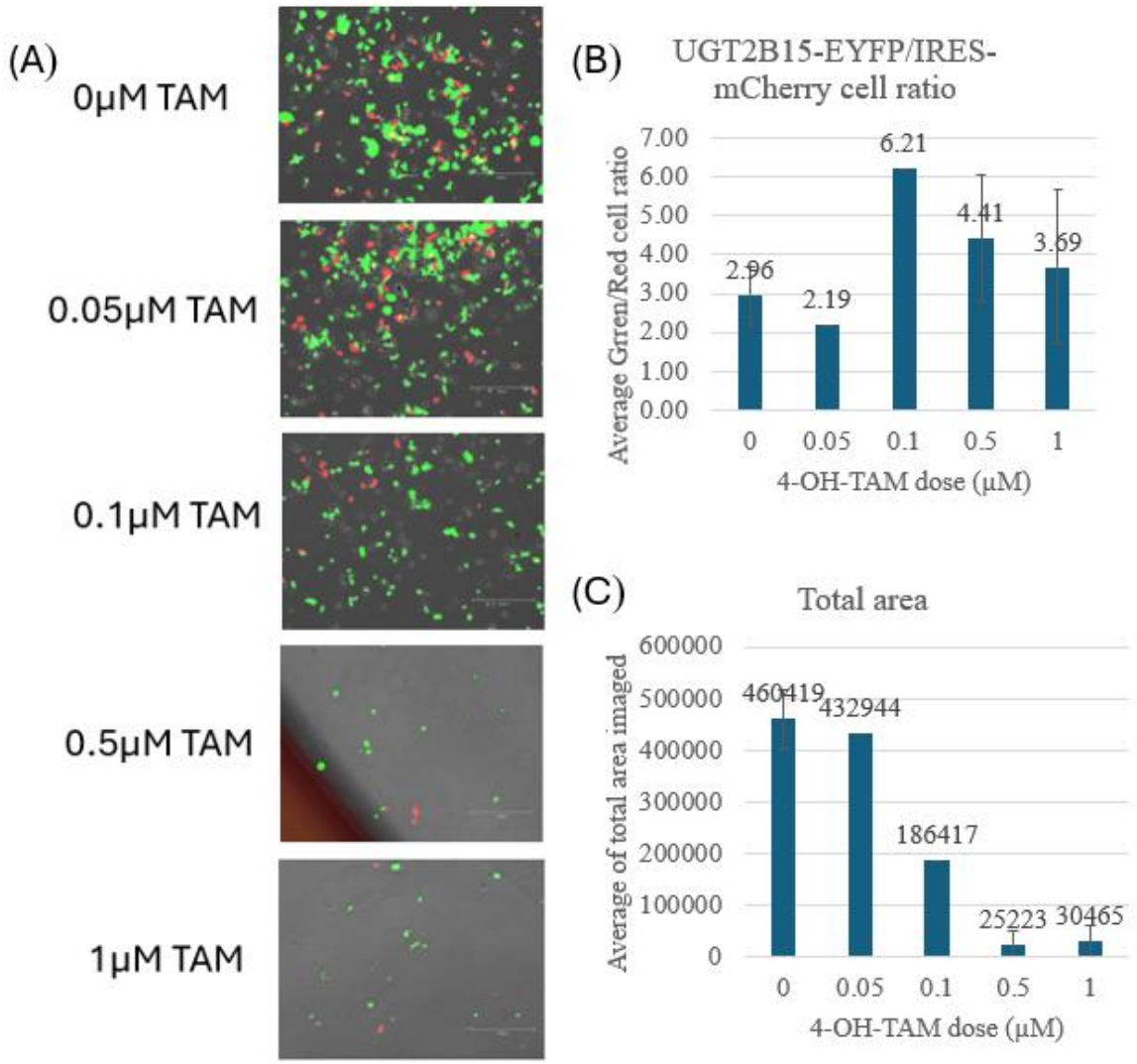

Figure 15. **Quantification of MCF7-UGT2B15-EYFP and MCF7-IRES-mCherry cells cultured at different doses of 4-OH-TAM**

(A) Representative images from fluorescence-based competition assay using combined populations of red MCF7-IRES and green MCF7-2B15 double stable cell lines at different doses of 4-OH-TAM. Images showing the growth of the green and red cells under increasing 4-OH-TAM doses- 0, 0.05, 0.1, 0.5, and 1μM. At 0μM after 3 weeks of treatment. There was a dramatic reduction in the total number of cells at the highest doses of 4-OH-TAM. Images were captured using EVOS-FL cell imaging microscope under 2X magnification.

(B) Ratio of green to red cells at each dose of 4-OH-TAM.

(C) Total cell area at each dose of 4-OH-TAM. Data in Panels B and C were generated by quantifying the masked cell area in images taken using the EVOS-FL red or green filter sets in replicate wells using ImageJ, further analysis was performed using Excel.

4 DISCUSSION

4.1 General overview of the study and its findings

Breast cancer is a prevalent and challenging disease, with 1 in 7 women diagnosed in their lifetime. This disease is highly heterogenous with a number of subtypes that have radically differing outcomes and treatment strategies. ER+ breast cancer is usually treated with hormonal therapies which is focussed on estrogen signalling pathways that fuels the cells to become cancerous. Tamoxifen is most widely applied hormonal therapy in both premenopausal and postmenopausal, although postmenopausal women are treated with aromatase inhibitors as their first line hormonal treatment. This is due to estrogen being produced via aromatisation of androgens in fat tissues rather in ovaries. Around 70% of BC have androgen receptor as prospective target and evidence is also emerging that targeting AR can be advantageous in particular patient subgroups, especially those with ER+/AR+ tumours. Emerging clinical evidence suggests androgen therapy might supress the activity of ER and provide value in some patients but remains experimental and not yet standardised (Palmieri et al., 2024). One significant mode of resistance in any form of anti-cancer drug therapy, including the above-mentioned hormonal therapy is direct metabolism/ inactivation intratumorally. Here falls one interesting part of the current project which is intratumoral drug metabolism.

This research study looked into UGTs, that are drug metabolising enzymes responsible for glucuronidating steroids and steroidal activity rendering them inactive. My primary focus was on UGT2B15 enzymes, which are the enzymes expressed in ER+ breast cancer cells and one that can activate the active form of tamoxifen, 4-OH-TAM. The study approached to examine whether overexpression of UGT2B15 alters MCF7 cell's sensitivity through utilizing different sets of strategic experiments. Most of the experiments performed were planned for short term duration under short term transient overexpressing conditions of UGT2B15 such as the cell growth analysis and estrogen responsive gene expression analysis. These experiments were designed to rapidly assess the acute effects of UGT2B15 on cell proliferation and estrogen signalling. But the last bit of the project designed was for analysing the effect of long-term stable overexpression of UGT2B15 by using competitive growth assay using fluorescently tagged cell lines. Generally, some part of the study supported the hypothesis which concluded that UGT2B15 may participate in 4-OH-TAM resistance, and some experiments had indefinite outcomes and should be re-run. These studies require further research to elucidate the

mechanistic aspects and the possible clinical implications of inhibiting UGT2B15 in tamoxifen treated breast cancer. The main findings from current study are discussed below.

4.2 UGT2B15 overexpression increases resistance to tamoxifen

As demonstrated by the performed assay results across all doses of TAM, it is conclusive that MCF7 cells that had been transiently transfected with UGT2B15 were partially resistant to 4-OH-TAM when compared to the control IRES-transfected cells. The IRES-transfected cells showed a significant dose dependent decline in cell numbers with increasing drug doses (relative to the vehicle control). However, UGT2B15-transfected cells only showed a significant reduction in cells at the highest drug dose (1μM). This lowering of growth inhibition of the UGT2B15 overexpressing group is in accordance with hypothesis 1 that tells that the overexpression of UGT2B15 enzyme could increase resistance to 4-OH-TAM, hence inhibiting its growth inhibition ability. More experiments should be done to confirm these results. In addition to that, IC50 values should be obtained to accurately determine the level of resistance there is (Tseng et al., 2004). This will require additional assays as well as additional doses of drugs so that there will be a saturation of response at the high end of the dose range evicting maximal effect allow appropriate fitting of the expected curve in dose dependent graph construction.

The obtained results are overall consistent with the previous findings that UGT polymorphisms are associated with drug resistance during breast cancer therapy (Lazarus & Sun, 2010; Mazerska et al., 2016). It is however to our knowledge the first direct evidence that increasing the level of UGT2B15 in ER+ breast cancer cells can increase their resistance to 4-OH-TAM. Despite the additional work required to prove mechanism, these would suggest the association of high UGT2B15 expression in patient tumours with poor outcomes, may be due to its ability to inactivate the drug within the tumour cells itself. If this is the scenario, it might find potential use as a candidate biomarker for predicting the patient response to tamoxifen (Wang et al., 2024). Additionally, exploring UGT2B15 inhibitors might assist in optimising treatment strategy in breast cancer.

4.3 Construction of lentiviral transduction

One among the major goals of this research was to develop a long-term competitive assay to determine the impact of UGT2B15 on long term 4-OH-TAM responses (detail in section 4.5). An effective way to distinguish between the control and UGT2B15 overexpression cells was to mark them fluorescently with different coloured proteins (red fluorescent protein and green fluorescent protein used here). Lentiviral transductions was originally chosen because of its high efficiency and ability to integrate the transgenes into host genome stably (Curran et al., 2000). A set of bicistronic lentiviral vectors had been previously made for this purpose; one co-expressed EYFP with UGT2B15 and the other expressed mCherry with no downstream protein. Both vectors were also previously shown to be able to be packaged and generate virus that could transduce a different cell line (LNCaP). The packaging protocol was performed following standard procedure.

Despite high transfection efficiency in packaging HEK293T cells, the following transduction of the MCF7 cells were not effective from the observations under fluorescence microscopy. Various modifications were tried to optimise the experiments, such as altering the DNA: Lipofectamine ratio used, varying batches of packaging plasmids and changing stocks of polybrene, however none of these worked. And since I had time constraints, it was eventually decided to switch from viral to non-viral transfection approach to generate the cell lines necessary to perform the planned assay (see Section 4.5). The exact cause that underlies viral packaging issues were not clear; however, some checking the size and integrity of the packaging plasmids on an agarose gel, suggested that the gag-pol plasmid may have been structurally compromised. Therefore, a new copy of this plasmid has been purchased for future experiments.

4.4 Variability in gene expression analysis

PS2 is a well-known ERα target gene that codes for trefoil factor 1, which has roles in cell growth and is predominantly known in association with breast cancer. Additionally, it is serves as a predictive marker for good response to endocrine therapy in breast cancer (Corte et al., 2006). Brown et al. (1984) showed that pS2 mRNA in MCF7 cells was induced rapidly by the treatment of E2. It was later found that tamoxifen could supress the E2 mediated induction of PS2 mRNA in MCF7 cells (Westley et al., 1984). These characteristics made PS2 an ideal

exemplar gene for determining the anti-estrogenic activity of 4-OH-TAM. Pilot experiments (not shown) were performed to determine the optimal time of treatment with 4-OH-TAM and E2. This led to a treatment protocol wherein cells transiently transfected with either IRES or UGT2B15 plasmids, were given 2 days to recover and then treated with 4-OH-TAM for 3 days, and finally with E2 for 2 days. It was expected that in the UGT2B15 transfected condition, most of the 4-OH-TAM would be glucuronidated, thereby freeing the ERα to bind to E2. In contrast, in the IRES-transfected cells, the ERα would be occupied with 4-OH-TAM and unable to bind to E2.

The qRT-PCR assay results were not statistically significant due to high experimental variation between the biological replicates (n = 4). Therefore, these findings cannot support or refute the original hypothesis 2 regarding the influence of UGT2B15 on the direct anti-estrogenic effect of 4-OH-TAM. The experimental variations can have several causes. The RNA yield differed among various experiments performed, most probably because the cell densities differed. This may have been either due to technical error (for example, counting and seeding), or biological variabilities e.g. differences in health of cell stocks when seeded for the experiments. As an example, it was noticed that the cells harvested at 100% confluency as opposed to 80-90%, attached more poorly to the new plate. To ascertain if there was any variation in the degree of UGT2B15 overexpression, the abundance of UGT2B15 mRNA was estimated across 3 independent experiment's sets of RNA samples. Unexpectedly, the endogenous abundance of UGT2B15 mRNA under the IRES-transfection condition in the first experiment set was lower as compared to the second two sets. Variation among the endogenous UGT2B15 expression in MCF7 cells has been observed previously in this lab. It was not clear what reason underlies this, but endogenous expression of UGT enzyme can be regulated by cell density. In every experiment conducted, there was considerable level of UGT2B15 overexpressed in the UGT2B15 transfected cells (normalised to GAP-DH) but the fold change in induction over the endogenous level was extremely variable between the experiments. In this short-term transfection, control IRES transfection was supplemented with a small spike of GFP vector to facilitate transfection efficiency measurement by fluorescence microscopy. This suggested that transfection efficacy was generally no more than 60% with some variability between experiments (data not shown). Altogether the transfection efficiency could contribute to the intra-experiment variations.

Improvement of methodology, including standardisation of the cell density plating and further replication is needed. Further development of the current assay, for instance, the

possible use of other ER target genes and normalisation strategies may also help to differentiate these effects. Other classical ER target genes that could be included in this analysis include growth regulation by estrogen in breast cancer 1 gene (GREB1), which has important contribution towards hormone dependent cancers (Cheng et al., 2018; Haines et al., 2019). In addition, other ways to assess the effect of UGT2B15 on 4-OH-TAM activity may involve knockout/knockdown of the UGT gene using CRISPR or siRNA.

4.5 Pilot competition assay

A growth competition assay was developed that combined cells with and without UGT2B15 overexpression together and then permits them to be observed while competing for growth in the presence of different concentrations of 4-OH-TAM. This assay can better represent the situation in a natural tumour where:

a) Cells have heterogenous expression profiles, and some cells likely have much higher UGT2B15 expression than other cells
b) Tumours are exposed to active tamoxifen metabolites over a prolonged period of time

Among cancer patients, majority of the tumour regression is seen over the first 3 months of treatment. But TAM is usually prescribed for 5-10 years to prevent relapse. We expected that if cells with UGT2B15 overexpression have a growth/survival advantage that will allow them to outcompete the control cells to become the dominant for, over a period of weeks in culture (including multiple cell passages). The first approach to building the competition assay was to create new cell lines with bicistronic lentiviruses encoding the UGTs and fluorescent proteins (refer Section 2.3.2). However, because of packaging problems, the plan was changed. Rather than that, already available MCF7 stable cell lines containing the UGT2B15 and empty IRES vectors were revived from cryostorage, verified by immunoblotting and then used to generate 'double stable' cel lines by stably transfecting (inserting the genome) green and red fluorescent proteins vector. The original pIRES vectors were puromycin resistant, so fluorescence vectors resistant to neomycin were chosen.

All of the cell lines used in this study were derived from a bank of colonies generated after antibiotic selection. There were noted colonies that did not express fluorescence, which may be due to parts of the vector with the neomycin resistance gene but not the fluorescent protein gene being integrated into the genome. Most of these non expressors were removed

through scraping before all remaining fluorescence colonies were pooled together. The fluorescence microscopy analysis indicated that the pooled cells were expressing at high frequency. A pilot competition study was also conducted using the MCF7-UGT2B15-EYFP and MCF7-IRES-mCherry cells under 4-OH-TAM.

The protocol used for competition assay allowed for cells to grow under 4-OH-TAM treatment in steroid deplete media for one week, then trypsin detached and seeded fresh plates. After 2 days of recovery in standard growth media, cells were treated in 4-OH-TAM media for another week. Passaging the cells had two functions, firstly it avoided overgrowth of the untreated cells, secondly it imposed an extra selective pressure on the drug treated cells to be able to reattach onto the substrate. Although the pilot study possessed several limitations due to time constraints, e.g. cells imaged only at the final time point and not all conditions had images from replica wells, some useful findings existed. There existed a dose dependent reduction on cell numbers with a dramatic drop off at the highest 4-OH-TAM doses. This compiled with earlier research into the inhibitory effect on cell growth and pro-apoptotic functions of 4-OH-TAM. Green cells and red cells were quantified to determine if there was any drug dependent change in their ratio. This revealed that under the untreated (vehicle) condition, green cells exceeded red cells. This was unexpected and can suggest that either 1) that seeding of the cells were not equal through technical failure, or 2) green cells do grow faster than red cells constitutively (i.e. drug free). To be able to state which it is, the experiment must be repeated with microscopy imaging both at seeding time and during the experiment. There was minimal variation in the green: red ratio at the vehicle and 0.05μM dosage. Although there may have been a trend towards the higher green: red at the 0.1-1μM doses, due to the lack of replicates for the 0.1μM dose, and the very high variability in the different fields at the 0.5μM and 1μM dose, conclusion cannot be drawn from this. These pilot data are insufficient to test the third hypothesis that UGT2B15 overexpression can provide a long-term competitive growth or survival under 4-OH-TAM treatment.

To clarify the interpretation of the competition assay, appropriate controls must be included to overcome the potential confounding effects of the fluorescent proteins. One proposed option is to generate cell lines expressing the fluorescent proteins in isolation, for instance mCherry or EYFP, without the UGT fusion constructs. This would determine if either fluorophore itself has an impact on cell growth or viability. In addition, swapping the fluorescent proteins such as constructing UGT2B15-mCherry and IRES-EYFP cell lines would also ensure that any growth effects obtained are due to the UGT constructs and not due to

differential effects of the fluorescent proteins. These controls would ensure that differences in cell growth observed in the assay are due specifically to the expression of UGT and not due to labelling artifacts.

The competition experiment needs to be repeated with results optimised for sensitivity to detect modest variation in drug response. First, having equal number of cells plated on Day 1 is crucial. More lengthy experiments with several passages and imaging time points should be done in the future. Additional doses of the drug could be used to rigorously examine the competitive dynamics (particularly at lower doses). It would also be interesting to use 3D culture conditions such as non-adherent mammosphere culture, or organoids grown embedded in extracellular matrix such as Matrigel (Dhimolea et al., 2021; Hogstrom et al., 2023), as the microenvironment may influence the extent to which metabolism of 4-OH-TAM can provide a survival advantage.

4.6 Limitations and considerations for future studies

Some of the drawbacks of the studies have already been mentioned above and they give direction to future studies. Some other considerations for the enhancement of the experimental design are use of alternative cell growth assays for the drug sensitivity experiments in transfected cell lines. These may be the micro tetrazolium assays (MTT and MTS) that quantify cell metabolic activity (Alley et al., 1988; Scudiero et al., 1988), or real time cell imaging with an Incucyte (Lanigan et al., 2020). Another possibility is cell cycle analysis by a flow cytometer because tamoxifen has been shown to inhibit progression of cells from GO/GI to the S-phase in the cell cycle process. These assays may be applied in both the transiently transfected and stable transfected cell populations. Additional experiments such as IC50 determinations must be carried out to verify and measure the protective effect of UGT2B15.

Though the double stable cell lines have been produced to use in the competition assays, it would still be desirable to produce models which co-express the UGT and the fluorescent protein from a bicistronic vector. Since the two genes in a bicistronic vector are typically expressed at high equivalent levels, the intensity of the fluorescence can serve as a readout of the level of UGT expression. This may permit the amount of UGT expression to be linked with long term survival. Attempts to create such lines in this project using lentiviral vectors were unsuccessful due to poor transduction efficiency. Future investigations should try replacing the

packaging plasmids with new stocks, and also explore ways to improve efficiency, including treatment of cells with neuraminidase which is beneficial through alteration of the surface glycans generate such cell lines. Future versions of competition assays will also examine a broader treatment condition set including more passages and wider range of 4-OH-TAM as described in section 4.5. Inducible expression systems could also be used a valuable approach to precisely adjust the level of UGT made to ensure that it stays within the range seen in patients' tumours.

Gene expression analysis in this project yielded useful few data because high variability. Besides the improvement of the methods for RNA extraction and RT-PCR, another approach to studying the activity of the ERα is by luciferase reporter gene assays. A luciferase reporter gene that contain estrogen response elements (ERE) called ERE-TK-Luc is available in the laboratory. This binds ERα and shows transcriptional activation of the luciferase gene by E2. A pilot experiment was conducted in this project using this reporter vector. However, the transfection was not efficient, and no measurable luciferase activity, hence the results were not presented. A likely explanation for the absence of luciferase activity was that a forward transfection protocol was employed.

Though MCF7 cells are efficiently transfected using the reverse protocol, in the forward protocol it is has been found to be highly sensitive to cell density, being nearly completely inhibited when density is high (Nooti et al., 2023). Therefore, future research may attempt to enhance the efficiency of this assay by using reverse transfection of the luciferase vector. Another method to broaden the outcomes of the impact of UGT2B15 on ERα function could be RNA sequencing that may reveal changes in the full transcriptome (Nooti et al., 2023; Zucha et al., 2021).

One last drawback of the project was the fact that it was not possible to investigate the impact of the orthologous gene UGT2B17 on drug responses in breast cancer cells. The original intention was to investigate the impacts of both UGT2B15 and UGT2B17 on drug responses in parallel. Time constraints, led to the decision to concentrate on studies of UGT2B15. But, fluorescently tagged cell models to study UGT2B17 were developed in parallel with the fluorescently tagged MCF7 cells as outlined in Section 3.4. Briefly, previously established ZR-75 stable cell lines that contained the UGT2B17-pIRES vector or the control empty pIRES vector were recovered from cryostorage and the expression of UGT2B17 was validated by immunoblotting (Appendix 3) prior to being stably transfected with mCherry-pcDNA3 and

pEYFPN1 vectors. These lines have been cryopreserved for use in future research, which can include competition assays under androgen treatment to find out if UGT2B17 might diminish the effectiveness of androgen-therapy in breast cancer. These studies will utilise both the models, and the protocols already established in this project.

4.7 Clinical implications

The finding from our short-term growth assays, that UGT2B15 overexpression can enhance tamoxifen resistance in MCF7 cells justifies the initial proposal that this UGT would be valuable as biomarker i.e. quantifying UGT expression in tumours from patients may guide personalised therapy. UGT2B15 may also be a drug target with UGT activity inhibitors being utilised in combination therapy to overcome resistance. But to establish the potential of these options would be important to take the cell-based results into models that more closely simulate in vivo tumours and into clinical samples. Taking competition assay to 3-dimensional (3D) cell culture models will more closely simulate the microenvironment in tumour (Moghimi et al., 2023) and give more clinically relevant information. Patient derived tumour specimens can likewise be grown in vitro or utilised for the creation of xenografts in mice that reproduce the inherent heterogeneity of patient tumours (Derose et al., 2013). These studies may also apply UGT knockout or knockdown techniques to reproduce the effects of possible drug-based inhibition of the UGT. To date, there are no selective UGT2B15 inhibitors. However, since some other UGTs have been shown to induce drug resistance such as UGT1A4 that induces resistance to drug used for acute myelogenous leukemia (AML), there are attempts being made to identify UGT targeted drugs through structural analysis of the protein (Osborne et al., 2024). Overall, the confirmation of the role of UGT2B15 in an animal models are likely the most critical in determining translational significance.

An additional means by which to increase the clinical relevance of this study is to conduct further studies of the correlations of UGT expression with survival measures in clinical data. Up to now, only the TCGA-BRCA dataset has been analysed, revealing a significant negative correlation of UGT2B15 expression with survival in ER+/PR+ tamoxifen-treated patients, but no association between UGT2B15 and survival in patients treated with an alternative hormonal drug Anastrozole. Unfortunately, there are very few publicly available datasets that consist of gene expression data, clinical data, and drug treatment data. Nonetheless, finding suitable

datasets and investigating gene survival relationships is of utmost necessity to justify the clinical validity of our model.

4.8 CONCLUSION

The findings described in this study suggest the role of UGT2B15 in breast cancer drug resistance. It offers preliminary evidence to support the hypothesis of project that intratumoral UGT2B15 overexpression contributes to 4-OH-TAM resistance via metabolic inactivation. However, assay variability and the need for further replication mean that some findings are inconclusive. These constraints can overcome by dedicated short term follow up experiments and long-term investigations using other breast cancer models in order to fully elucidate the role of UGT enzymes in resistance. The study thus emphasizes on the complexity of drug resistance mechanisms and highlights the need for further investigation of intratumoral drug metabolism to inform future treatment strategies.

5 BIBLIOGRAPHY

Akhdar, H., Legendre, C., Aninat, C., & More, F. (2012). Anticancer drug metabolism: chemotherapy resistance and new therapeutic approaches. *Topics on drug metabolism*, *22*, 138-170. https://doi.org/10.5772/30015

Allain, E. P., Rouleau, M., Lévesque, E., & Guillemette, C. (2020). Emerging roles for UDP-glucuronosyltransferases in drug resistance and cancer progression. *British Journal of Cancer*, *122*(9), 1277-1287. https://doi.org/10.1038/s41416-019-0722-0

Alley, M. C., Scudiero, D. A., Monks, A., Hursey, M. L., Czerwinski, M. J., Fine, D. L., Abbott, B. J., Mayo, J. G., Shoemaker, R. H., & Boyd, M. R. (1988). Feasibility of drug screening with panels of human tumor cell lines using a microculture tetrazolium assay. *Cancer Res*, *48*(3), 589-601.

Bock, K. W. (2016). The UDP-glycosyltransferase (UGT) superfamily expressed in humans, insects and plants: Animal□plant arms-race and co-evolution. *Biochemical Pharmacology*, *99*, 11-17. https://doi.org/https://doi.org/10.1016/j.bcp.2015.10.001

Bray, F., Ferlay, J., Soerjomataram, I., Siegel, R. L., Torre, L. A., & Jemal, A. (2018). Global cancer statistics 2018: GLOBOCAN estimates of incidence and mortality worldwide for 36 cancers in 185 countries. *CA: A Cancer Journal for Clinicians*, *68*(6), 394-424. https://doi.org/10.3322/caac.21492

Brown, A. M., Jeltsch, J. M., Roberts, M., & Chambon, P. (1984). Activation of pS2 gene transcription is a primary response to estrogen in the human breast cancer cell line MCF-7. *Proceedings of the National Academy of Sciences*, *81*(20), 6344-6348. https://doi.org/10.1073/pnas.81.20.6344

Cai, J., Huang, F., Gao, W., Gong, T., Chen, H., & Liu, Z. (2023). Androgen Receptor/AP-1 Activates UGT2B15 Transcription to Promote Esophageal Squamous Cell Carcinoma Invasion. *Cancers*, *15*(24), 5719. https://doi.org/10.3390/cancers15245719

Cerami, E., Gao, J., Dogrusoz, U., Gross, B. E., Sumer, S. O., Aksoy, B. A., Jacobsen, A., Byrne, C. J., Heuer, M. L., Larsson, E., Antipin, Y., Reva, B., Goldberg, A. P., Sander, C., & Schultz, N. (2012). The cBio cancer genomics portal: an open platform for exploring multidimensional cancer genomics data. *Cancer Discov*, *2*(5), 401-404. https://doi.org/10.1158/2159-8290.Cd-12-0095

Chanawong, A., Hu, D. G., Meech, R., Mackenzie, P. I., & McKinnon, R. A. (2015). Induction of UDP-Glucuronosyltransferase 2B15 Gene Expression by the Major Active Metabolites of Tamoxifen, 4-Hydroxytamoxifen and Endoxifen, in Breast Cancer Cells. *Drug Metabolism and Disposition*, *43*(6), 889-897. https://doi.org/10.1124/dmd.114.062935

Cheng, M., Michalski, S., & Kommagani, R. (2018). Role for Growth Regulation by Estrogen in Breast Cancer 1 (GREB1) in Hormone-Dependent Cancers. *International Journal of Molecular Sciences*, *19*(9), 2543. https://doi.org/10.3390/ijms19092543

Corte, M. D., Tamargo, F., Alvarez, A., Rodrã-Guez, J. C., Vã¡Zquez, J., Sã¡Nchez, R., Lamelas, M. L., Gonzã¡Lez, L. O., Allende, M. T., Garcã-A-Muã±Iz, J. L., Fueyo, A., & Vizoso, F. (2006). Cytosolic levels of TFF1/pS2 in breast cancer: their

relationship with clinical–pathological parameters and their prognostic significance. *Breast Cancer Research and Treatment*, *96*(1), 63-72. https://doi.org/10.1007/s10549-005-9041-7

Court, M. H. (2010). Interindividual variability in hepatic drug glucuronidation: studies into the role of age, sex, enzyme inducers, and genetic polymorphism using the human liver bank as a model system. *Drug Metab Rev*, *42*(1), 209-224. https://doi.org/10.3109/03602530903209288

Craig, W. A. (1998). Pharmacokinetic/pharmacodynamic parameters: rationale for antibacterial dosing of mice and men. *Clinical infectious diseases*, *26*(1), 1-10.

Curran, M. A., Kaiser, S. M., Achacoso, P. L., & Nolan, G. P. (2000). Effi duc Nond Opti ized u fi Virus Vect *Molecular Therapy*, *1*(1), 3 tps://doi. g/1 / 1999.

Dean, L. (20 apy nd UG ype In V. Pratt, S. A. Scott, Pirmohamed, B Esquivel, B L. Ka an, & A J.), *Medical Genetics Summaries*. Na (US

Der e, Y. ., h, K. M., Wang, ., las, A., an, P., Courdy, J., Welm, L., & Welm, Patient-Deriv Hum er: Pr In Vitr In Viv Applic Tumo *Current Protocols in Pharmacology*, *60*(tps://doi. g/10 2/04 .ph1

Dhimolea, ., s, ., Kans a, D., Al'Khafaji, ., Bouy ou, J., Weng, X., a, S., aja, J., te, P., aki, ., ang, H., ner, B. J., Liu, Z., ao, D., n, J., r, ., h, J., heffer, M., Je ohn, R.,...Mits s, Diapaus like Adapt h Suppress Tumo Per *Cancer Cell*, *39*(2), tps://doi. g/https://d g/10 6/j.

l Debs, B. W., Tschule , U., Griffiths, A. D., & en, mpetit cultiva er Drug Specific u *Journal of Biomolecular Screening*, *16*(8), 8 tps://doi. g/10 7/1 898

r, M. C., & Jacobs, T. oxif n *StatPearls*. tPearls Publis

Copyr © 4, tPearls Publis LLC tps://w v/books/NBK532905/

ao, J., Aksoy, B ., Dog usoz, U., D dner, G., Gr s, B., Sumer, S ., Sun, Y., Jac en, ., inha, ., Lar on, E., i, E., er, C., & u z, N mplex al Profiles Usi ioPo *Science Signaling*, *6*(269), pl1-pl1 tps://doi. g/10 6/s

er, R. L., & Dimit akakis, educ ubcutaneous one, ozole: prospe e, u *Maturitas*, *76*(4), 49. tps://doi. g/10 6/j. tur

Gonçalv s, H., Guerra, ., Duar a, J. ., er, V. ., um, I. V., & Bu eixeira, Sur tudy iple-Ne Non–Triple-Ne azili *Clinical Medicine Insights: Oncology*, *12*, 795 491 790 ttps://doi g/10 7/11795 491 790

s, C. N., Klin ith, H. D., & Burd, C. J. 19) u p ecept positiv oug odulation PI3K/Akt/ *bioRxiv*, tps://doi. g/10 1/7

n, W. ., engupta, S., & Katzene en, gulat
lucu z e UG eceptor-positiv
Endocrinology, *147*( ), 3 tps://doi. g/10 0/en.
an, F., ed, ., ti, ., on, ., & Yousif, toxic
effect oxif *Journal of Unexplored Medical Data*,
3(2), tps://doi. g/10 7/2
ckey, ., elth, L. A., a, K. M., Lav -Law, G., Milioli, H. H., oden, D., Jindal, S.,
u , M., u z, J., ie, E., Birrell, S. N., loo, S., o, R.,
x ou, ., , ., h, T. M., Ellis, I. O., Zwart, W., Palm i,
,... ey, W. D. eceptor is a tumor suppress
ecept –p *Nature Medicine*, *27*(2),
tps://doi. g/10 8/s 591
om, J. ., Cruz, K. A., S s, L. M., Ward, M. N., Mehta, T ., Kana ek, N., Philips,
J., Di i, V., Wulf, G., lins, L. ., Patel, J. M., & Muranen,
imultaneous epto –p
fibr *Journal of*
Biological Chemistry, *299*(8),
tps://doi. g/https://d g/10 6/j.jbc
Hu, D. G., I., P., Julie nn, H., A., ., & h, Regulatio hum
UDP- (UG iRNA *Drug Metabolism Reviews*,
54(2), 1 tps://doi. g/10 0/0
Hu, D. G., i, ., Hulin, J. ., McKinnon, ., Mackenzie, P. I., & h,
u L ape of UDP- (UG Hum
Cancers, *14*( ), 5 ttps://doi. g/10 390/c
Hu, D. G., i, ., Mackenzie, P. I., Hulin, J. ., McKinnon, ., & h,
Expr ion Profile Der u UDP ase (UGT)
Hum Outc *Cancers*, *13*(17),
491 tps://doi. g/10 390/c 491
Hu, D. G., Selth, L. A., T ulli, ., Meech, R., Wijayakuma a, D., Ch ong, A., Russell,
., ldas, C., on, J. L. L., l, J. ., ley, W. D., Mackenzie, P. I., &
ckey, ecept
u Hum UDP-Glu urono *Cancer*
Research, *76*(19), 5 893 tps://doi. g/10 8/0
u er, F. W., Barker, H. ., Lipert, B., hé, F., t, G., Pic t, J.,
iriou, C., & Jam on, S trastuzuma
-DM1 -pos *British Journal of Cancer*,
122(5), tps://doi. g/10 8/s 19-
u , N *The Cancer Genome Atlas (TCGA)*. Na titute
ps:// v/tc
Kaur, G., Gupta, K., h, P., Ali, V., Kumar, V., & Verma, M. (2020). Drug-metabolizi
enzymes: rug er. *Clinical and Translational Oncology*,
22(10), tps://doi. g/10 7/s12094-02
Kisanga, E ., Gje e, J., Guerr Gonzaga, A., Pig o, F., Pe i, A., R on, C.,
ano, D., Pelosi, G., Decensi, A., & Lien, oxif
erum ue during Three Dose
ized Preoper al. *Clinical Cancer Research*, *10*(7),
tps://doi. g/10 8/10

Krauß, J., & her, Pha okine)—E Drug De nzym *Scientia Pharmaceutica*, *86*(4), tps://doi. g/10 390/s iphar

Labo s, *Western Blotting: Electrophoresis Techniques*. Labo ://w om/en-au/applic s/w oph hniques?ID=PQEENTWDLBV5

Lanigan, M., u , M., Weber, D. P., Athukorala, K. S., mpbell, P. L., Fox, D. ., & Ruth, J. u z th, surviv pr u flu u ® *J Biol Methods*, *7*(2), e1 tps://doi. g/10 0/jbm.20

Lazarus, P., levins-Pr eau, ., Zheng, Y., & Sun, D. 09). Potential Role of UG Phar Pr . *Annals of the New York Academy of Sciences*, *1155*(1), 99- tps://doi.org/10.1111/j.1749-09. .x

Lazarus, P., & Sun, D. . Pot of UGT pha and prevention: u oxif *Drug Metabolism Reviews*, *42*(1), 1 194 tps://doi. g/10 09/03 090

Lippman, M., n, ., & Huff, K. (197 hum ue culture *Cancer Treat Rep*, *60*(10), 29.

Liu, W., Li, J., Zhao, ., Lu, Y., & uang, P. Ur diphospha (UDP) (UG super ily: t le in tumo *Front Oncol*, *12*, tps://doi g/10 89/f

Liu, W., Li, J., Zhao, ., Lu, Y., & uang, P. Ur diphospha (UDP) (UG super ily: tum *Frontiers in Oncology*, *12*. tps://doi. g/10 89/f

Livak, K. J., & S en, T. D. expr data using e quan e PCR -Delta Delta od. *Methods*, *25*(4), ttps://doi.org/10 6/m

ino, M., Jamal, Z., & Zito, P. *Pharmacodynamics*. tPearls Publishing, u L tp://europepm g/abs t/MED/299395

tp://europepm g/books/NBK50 791

tps://w v/books/NBK50 791

tin, Q.

ana, F., ta, ., Pavone, ., ta, L., la, S., Vitale, S. R., Manzella, L., & Vigneri, P. AKT s: New Weapon er? *Frontiers in Pharmacology*, *12*. tps://doi. g/10 89/fpha

Mazerska, Z., Mróz, A., Pawło ska, M., & Augustin, E. lucuronida drug *Pharmacology & Therapeutics*, *159*, tps://doi. g/https://d org/10.1016/j.pha 09

h, R., Hu, D. ., McKinnon, ., u okah, N., s, Z., Nair, P. C., d, ., & Mackenzie, P. 19) UDP- e (UGT) Super ily: New s, New u , nd No el Par *Physiol Rev*, *99*(2), 1 tps://doi. g/10 2/phy

himi, N., ni, ., Dalan, ., ezaei, D., an, A., & Kohandel, tum ultur 3D

-pr u p *Scientific Reports*, *13*(tps://doi. g/10 /s4159 -x

Na ound *Breast Cancer stats in Australia*. tps://nbc au/abou er/br tats/

Nooti, S., Naylor, M., Long, ., l, ., & u LucFlow: easur Luc epor expr *PLOS ONE*, *18*(10), e0292 tps://doi. g/10 1/journal.pone 292

u , E., -Nuñez, P., Acuña u , L. E., Gómez-V s, ., & írez-V spino, C u p (pp. Exon Public ps:// / 5/exon-public u p

ne, J., ulekha, A., Culjk -Kraljac c, B., ek, J., Rue er, E., Jo u , ., r, A., u , S., & den, K. L. NMR Dr en Dis N el UDP- u uron apeutic *Journal of Molecular Biology*, *436*(2), tps://doi. g/https://doi. g/10 6/j.jmb

Palm i, C., Linden, H., B l, S. N., Wh ht, S., Lim, E., S tzberg, L. S., Dw er, ., ckey, ., ugo, ., bb, P., O'S u y, J. ., Jo n, S., u ky, A., ey, W. D., & er, m, el, al, ecept u , ecept positive, oe ecept -positive, and u : ed, open label, u e, u *The Lancet Oncology*, *25*( ), 3 tps://doi. g/10 6/s

Pa a, S., tia, ., aldi, ., h, ., & l, R. K. Drug olizing enzyme s' *Biomedicine & Pharmacotherapy*, *105*, tps://doi. g/https://d g/10 6/j.bioph

Perou, M., Sørlie, T., en, ., Van De ijn, M., Jeffrey, ., s, C. A., Pollack, J. ., R s, D. ., Jo en, H., Akslen, L. ., Fluge, Ø., Per chikov, A., Wil s, ., Zhu, X., Lønning, P. ., Bør -Dale, A.-L., wn, P. O., & Bot tein, D. u p u tu urs. *Nature*, *406*(6797), tps://doi. / 8/35 9

Phan -Lyn, S., & Lle na, V. y, In *StatPearls*. tPearls Publis

ao, X., Huang, X., Zhou, Z., & Lin, X. impr 2ˆ(for quant poly *Biostat Bioinforma Biomath*, *3*(3), 7

d, A., s, J. O., & ckenzie, P. UDP-glucuronosyltransferases: drug detoxific n. *The international journal of biochemistry & cell biology*, *45*( ), 1

d, A., s, J. O., & ckenzie, P. UDP-glucuronosyltransferases: drug detoxific *Int J Biochem Cell Biol*, *45*(6), tps://doi. g/10 6/j. 19

ozeboom, B., Dey, N., & De, P. (19) ER+ m er: past, pr ent, and a pr iptio apopto u ure *Am J Cancer Res*, *9*(12),

ific, ulture P
tps://w ofis om/au/en/home/r s/g ultur
basics/c ulture p ols/c ulture u eful-num
ific, eezing
tps://w ofis om/au/en/home/r s/g culture
basics/c ulture p ols/freezing
ific,
tps://w ofis om/au/en/home/r s/g culture
basics/c ulture p ols/th
u , D. A., aker, . H., Paull, K. D., Monks, ., ney, ., Nofziger, .,
u , J., eniff, D., & Boyd, M. 198 lua oluble
azolium/f azan drug ultur using
hum umor *Cancer Res*, *48*( ),
u , L., bner, ., & u hell, B. (1993). expr UDP-
u ur e UG u k
spon u *Biochem Pharmacol*, *45*(2), 295
tps://doi. g/10 6/00 295 (93)90
eng, E., ay, ., & is, Die
toxic in Human Epith
Line *Experimental Biology and Medicine*, *229*(8),
tps://doi. g/10 7/15 290
Tukey, H., & u , P. u UDP-glu urono s:
m, expr ion, *Annu Rev Pharmacol Toxicol*, *40*,
tps://doi. g/10 6/annurev.p tox.40
Waks, ., & Winer, P. 19) ent: *JAMA*, *321*(3),
ttps://doi. g/10 1/jama 193
Walsh, A. J., ok, ., s, ., u hio, L., o, G., a, C. L., &
Skala, Quant Optic Primary Tumor
Pr Drug spon *Cancer Research*, *74*(18),
194 ttps://doi. g/10 8/0
Wang, C., ai, C., Zhang, Z., Zhou, H., ao, H., Wang, S., & Yuan, Y. UG
-po spo tuzuma affec
epitheli ition: A pot arker y pa
tuzum ent. *Cancer Gene Therapy*, *31*( ),
tps://doi. g/10 8/s 19-
Wang, J., & Wu, er: u peu
s, lenge, Perspec *Breast Cancer: Targets and Therapy*,
Volume 15, 7 tps://doi g/10 7/bc
Westley, B., May, F. ., wn, M., Krust, ., bon, P., Lippman, ., & t,
198 Effec u p RNA
-ki pr x subline
Journal of Biological Chemistry, *259*( ),
tps://doi. g/https://d g/10 6/S -92)9092
Yang, X. R., an, ., imm, D. L., Lis ska, J., n, L. A., Peplonska, B.,
t, ., on, W. F., Szeszeni -DąB ska, N., -Mikolajczak, A.,
Za nski, W., u , R., h, D., ymki cz, G., Ligaj, M., Lukaszek, S.,
Kordek, ., & í as, Differ isk Fac

u ubtyp a Populat u *Cancer Epidemiology, Biomarkers & Prevention*, *16*(3), 39- ps://doi.org/10.1158/ 9965.epi-06

Yur henko, P. O., hkarupa, V. M., Kac ula, ., Kakarkin, Y., Ko huk, P., Ko huk, P., Pech tiy, M., & hukov, D. Influenc poly orphis enzy UDP lucurony oxif apy lumina *Reports of Vinnytsia National Medical University*, *27*( ), tps://doi. g/10 393/repor

Zahreddine, ., uljk -Kralja ic, ., u , S., on, P., eo, ., is, J., ck, ., Jaquith, J. ., i, L., olakis, E., i, A., on, J., Leber, B., Becker, M. W., Pei, S., Jordan, C ., M ler, W. H., & B en, K. L. r GLI1 impa drug ough u lucu *Nature*, *511*( ), 90-93 ps://doi.org/ 8/na u

Zucha, D., Kubista, M., & Valih h, L. u : Gu qPCR. *Cells*, *10*(10), 2 tps://doi. g/10 90/

6 APPENDICES

6.1 APPENDIX 1

6.1.1 List of chemical reagents along with supplier companies

Chemicals	**Supplier company**
Dulbecco's Modified Eagle Medium (DMEM)	Life Technologies, Victoria, Australia
Roswell Park Memorial Institute (RPMI) Medium 1640	GIBCO
Phosphate Buffered Saline (1xPBS)	Life Technologies, Victoria, Australia
Foetal Bovine Serum (FBS)	Sigma-Aldrich, Saint Louis, United States
Trypsin	Life Technologies, Victoria, Australia
Ethanol (70%, 80%, 100%)	Chem Supply, South Australia, Australia
DMSO Freezing media	* 6.1.2
Lipofectamine ® 2000	Invitrogen (Life Technologies)
Serum free RPMI	GIBCO
Plasmid	Promega
TRIzol reagent	ThermoFischer Scientific
Chloroform	Chem Supply, South Australia, Australia
Nuclease free water	Promega, USA
Isopropanol	Chem Supply, South Australia, Australia
Glycogen 20mg/mL	Sigma-Aldrich
DNase	Life Technologies, Victoria, Australia
DNase buffer	Life Technologies, Victoria, Australia
EDTA 25mM	Sigma-Aldrich, Saint Louis, United States
Deoxynucleotide-triphosphate (dNTPs) 10mM	Life Technologies, Victoria, Australia
Random hexamers	Life Technologies, Victoria, Australia
Reverse transcriptase buffer	Astral Scientific, New South Wales Australia
RNase inhibitor	Astral Scientific, New South Wales

	Australia
NexGen® M-MulV Reverse transcriptase	Astral Scientific, New South Wales, Australia
GoTaq qPCR master mix	Promega, USA
PS2 gene primers	Macrogen
GAP-DH gene primers	Macrogen
0.5% Crystal violet	ThermoFischer
50% Methanol	Chem Supply
Charcoal stripped serum (CSS)	Sigma
Estradiol	Sigma

6.1.2 Composition of important media & laboratory reagents

DMEM Media Sodium Pyruvate 5% 100X MEM Non-essential amino acids 5% 10,000units/mL Pen Strep 5 ml	**Crystal Violet Staining Solution (0.5%)** Crystal violet powder 0.5 g Distilled H_2O 80 mL Methanol 20 mL
DMSO Freezing Media DMSO 90% FBS 10%	**0.2µg/mL Puro** 25mL RPMI 0.5mL Puromycin
1 x (PBS) NaCl 137Mm Na_2HPO4 10 Mm KCL 2.7 Mm KH_2PO_4 2 Mm Ph 7.4	**400µg/ml G418** 40mg G418 (Geneticin) 100mL RPMI
Acrylamide gel 1M Tris pH 8.8 40% Acryl/Bis 20% SDS	**Stacking gel** 1M Tris pH 6.8 40% Acryl/Bis 20% SDS

10% APS Temed Nuclease free water	10% APS Temed Nuclease free water
SDS loading dye 1M Tris Glycerol SDS 2-β-mercaptoethanol Bromophenol blue Nuclease free water	**Elution buffer** 20 mM Tris 5 mM EDTA 50 mM NaCl 1% SDS pH 8.0
TE Buffer 1mM EDTA 10mM Tris pH 8.0	**SDS-PAGE running buffer** 25mM Tris 192mM Glycine 0.1% SDS pH 8.3
Tris Buffered Saline (TBS) 10mM Tris 150mM NaCl pH 8	**SDS-PAGE transfer buffer** 25mM Tris 192 mM Glycine 20% Methanol pH 8.0
TBST 0.5M Tris 1.5M NaCl 2.5L Nuclease free water 0.2% Tween 20	**Blocking in 3% non-fat milk powder** 50mL TBST 3% Skim milk powder

6.1.3 Consumables

Consumable	Manufacturer
Nunc™ Cell-Culture Treated Multi-dishes (6 wells, 12 wells, 24 wells, 96 wells)	Thermo Fisher Scientific™
Serological Pipettes	Sarstedt, South Australia

(2 ml, 5 ml, 10 ml, 25 ml)	
Centrifuge Tubes (10 ml, 50 ml)	Sarstedt, South Australia
Micro Tubes (0.5 ml, 1.5 ml)	Sarstedt, South Australia
Barrier tips	Edwards
Nunc™ EasYFlask™ Cell Culture Flasks with filter cap (25 cm^2, 75 cm^2, 175 cm^2)	Thermo Fisher Scientific™
PCR Tubes (0.1 ml)	Corning® Axygen®
Cryo Tubes (1ml, 1.5ml)	Sigma-Aldrich
Sterile aerosol barrier tips 10 µL, 200 µL, 1250 µL	Edwards

6.1.4 Technical apparatus

Apparatus	**Manufacturer**
Rotor- Gene Q Real Time PCR	Qiagen Rotor-gene Q
NanoDrop One - Micro-UV/Vis Spectrophotometer	Thermo Fisher Scientific™
Laminar Flow Hoods	DynaFlow 1500GRP
Brightfield Inverted Microscope	Zeiss Primovert
Haemocytometer	Hausser Scientific
Biosafety Cabinet	HERAsafe and MAXISAFE 2030i
ChemiDoc	Bio-Rad
CellDrop™ Automated Cell Counters	CellDrop (Deno Vix)
Incubators	PHCbi
Mini centrifuge	Sarstedt
PCR Cabinet	Aura PCR
Centrifuge	Thermo Scientific Mega Fuge 8R
Bead bath	Thermo Fischer Scientific
Pipettes (P2, P20, P200, P1000)	Interpath
Pipette gun	Thermo Fisher Scientific™

EVOS® FL Cell Imaging Microscope	Thermo Fisher Scientific™
Multi-channel pipette	Eppendorf
Liquid Nitrogen Freezer	PHCbi
Vortex mixer	Sigma Aldrich
DNA Thermal cycler	Perkin Elmer Cetus
Microplate scintillation &luminescence counter	Packard
CO_2 thermoregulatory incubator	ThermoFischer

6.1.5 Computational Software

Software	**Use in the current study**
Microsoft® Excel®	Result calculation for RNA Assay
Id 5 software version 1.2.0.0	Plate reading for Growth Assay
NanoDrop One - Micro-UV/Vis Spectrophotometer	Determining RNA concentrations in the samples
Qiagen Rotor-gene Q software 2.3.4	qRT-PCR result analysis
EVOS® FL Cell Imaging Microscope	Fluorescence microscopy for cell imaging
Lab scope imaging software	Imaging of cell culture plates and individual wells
Cell Drop™ Automated Cell Counter	Counting the number of cells in the sample
Bio-Rad Chemidoc v3.0.1	Imaging the gel
CBioPortal	Clinical data analysis
R Studio console 4.5.0	Results analysis for finding statistical significance

6.2 APPENDIX 2

6.2.1 Plasmids

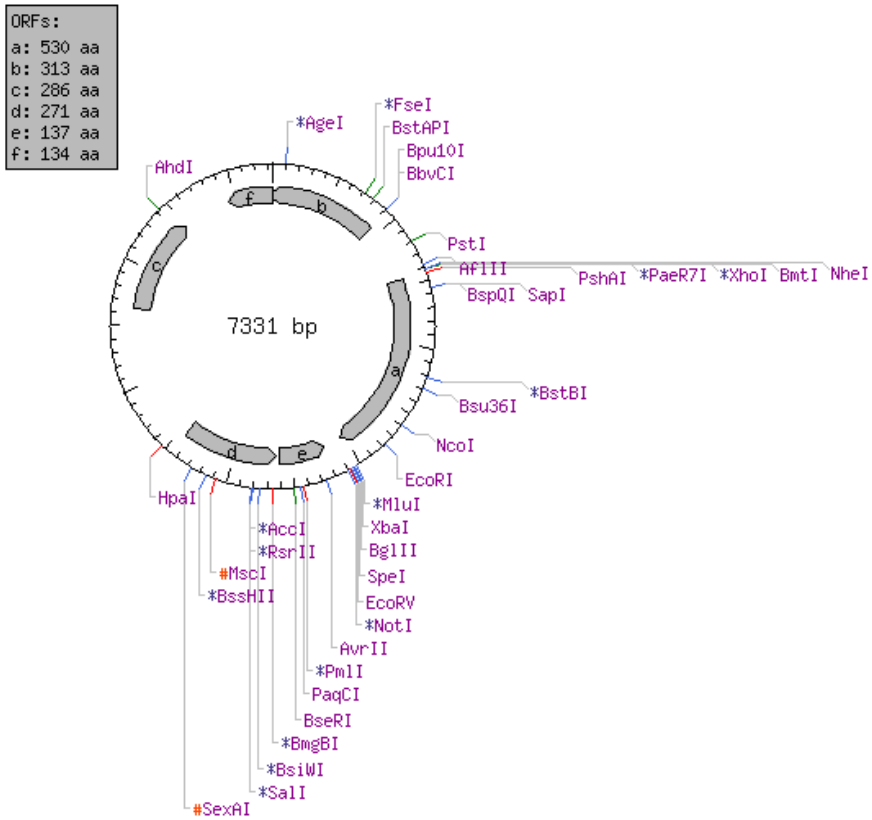

Figure 16. **Plasmid map of wild type 2B15 [UGT2B15-pIRES]**

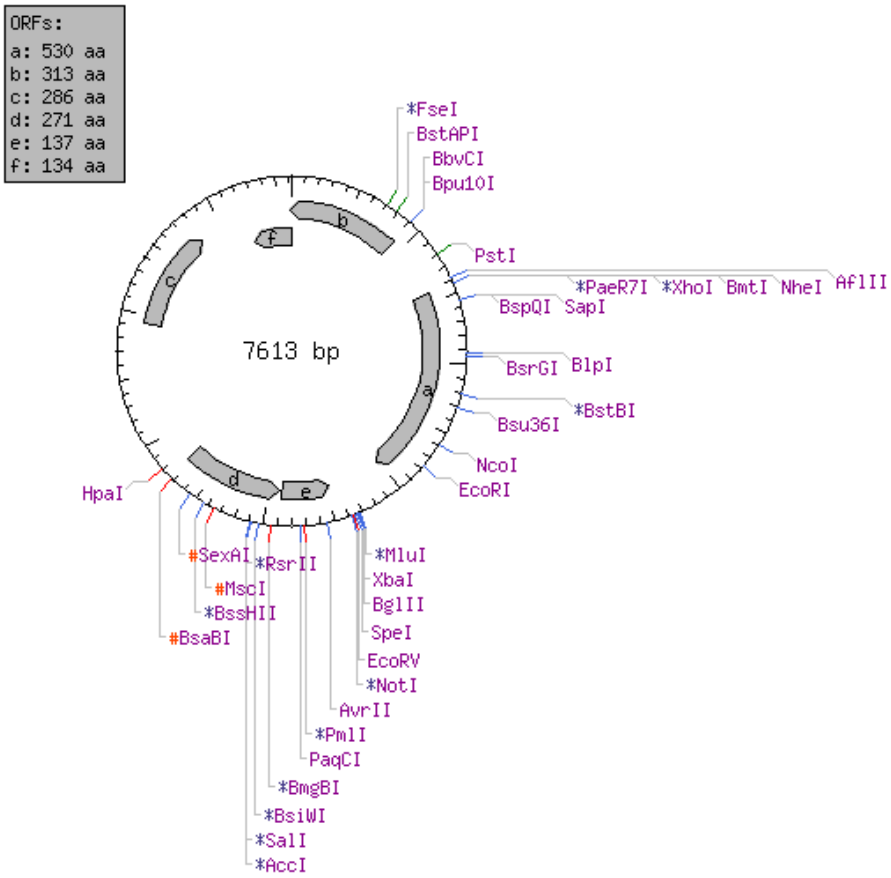

Figure 17. **Plasmid map of wild type 2B17 [UGT2B17-pIRES]**

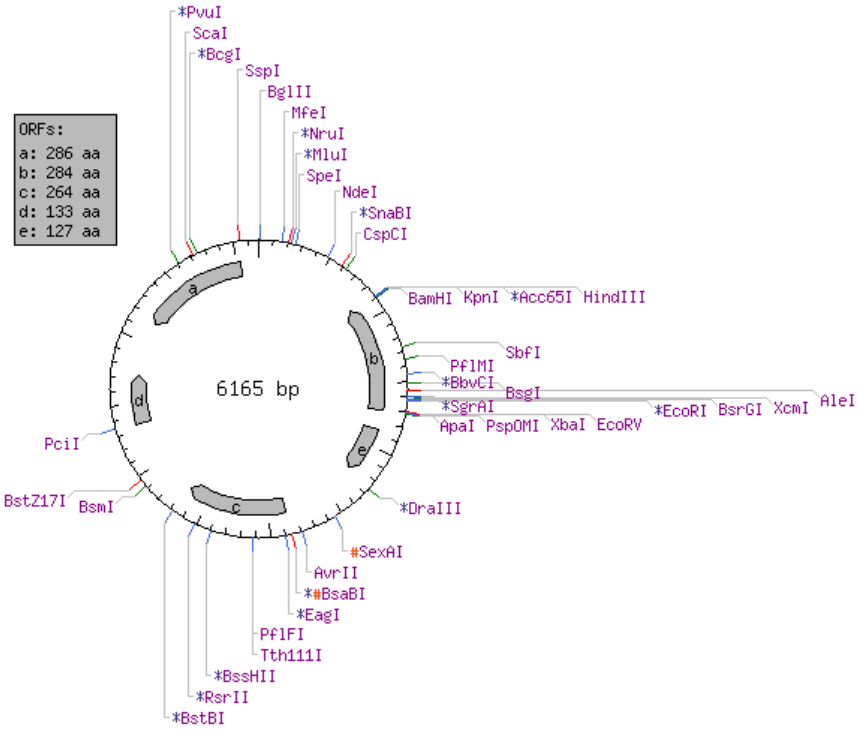

Figure 18. **Plasmid map of mCherry-2A-pcDNA3**

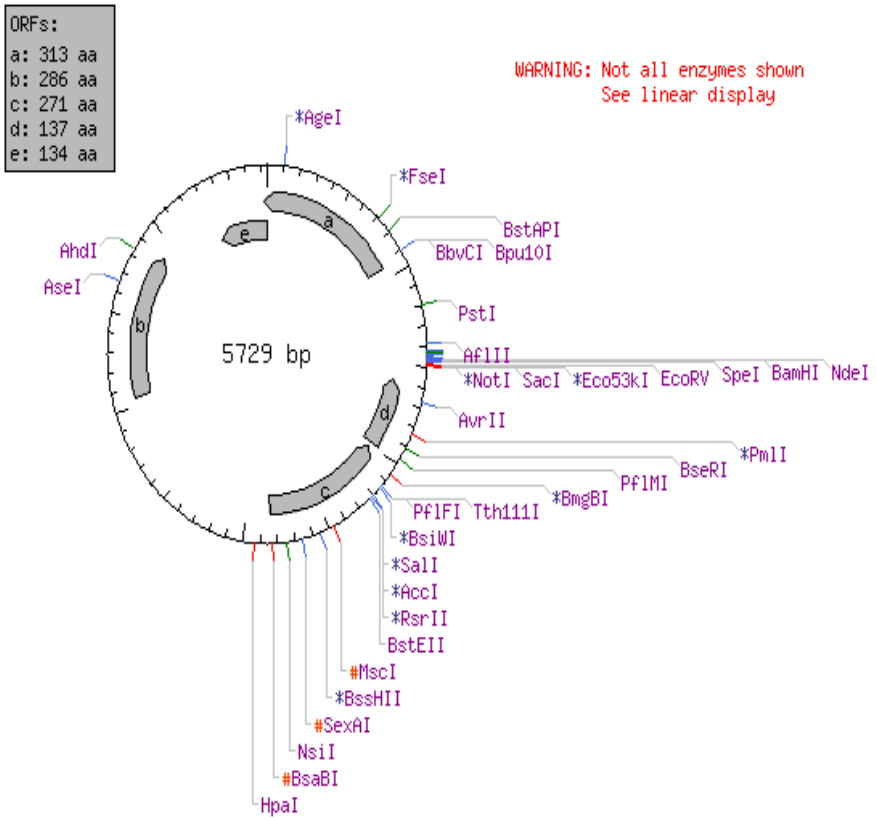

Figure 19. **Plasmid map of pEYFPN1**

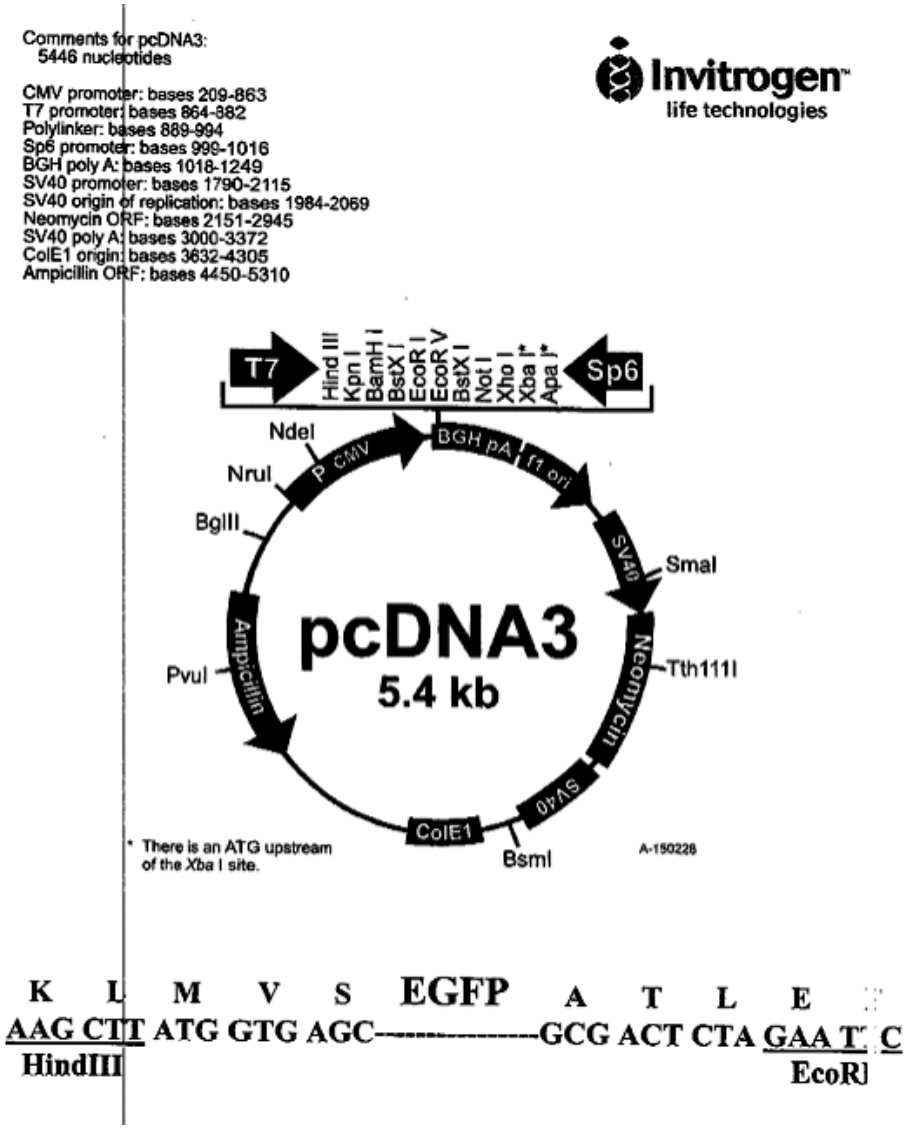

Figure 20. **Plasmid map of mCherry-2A-pCDNA3**

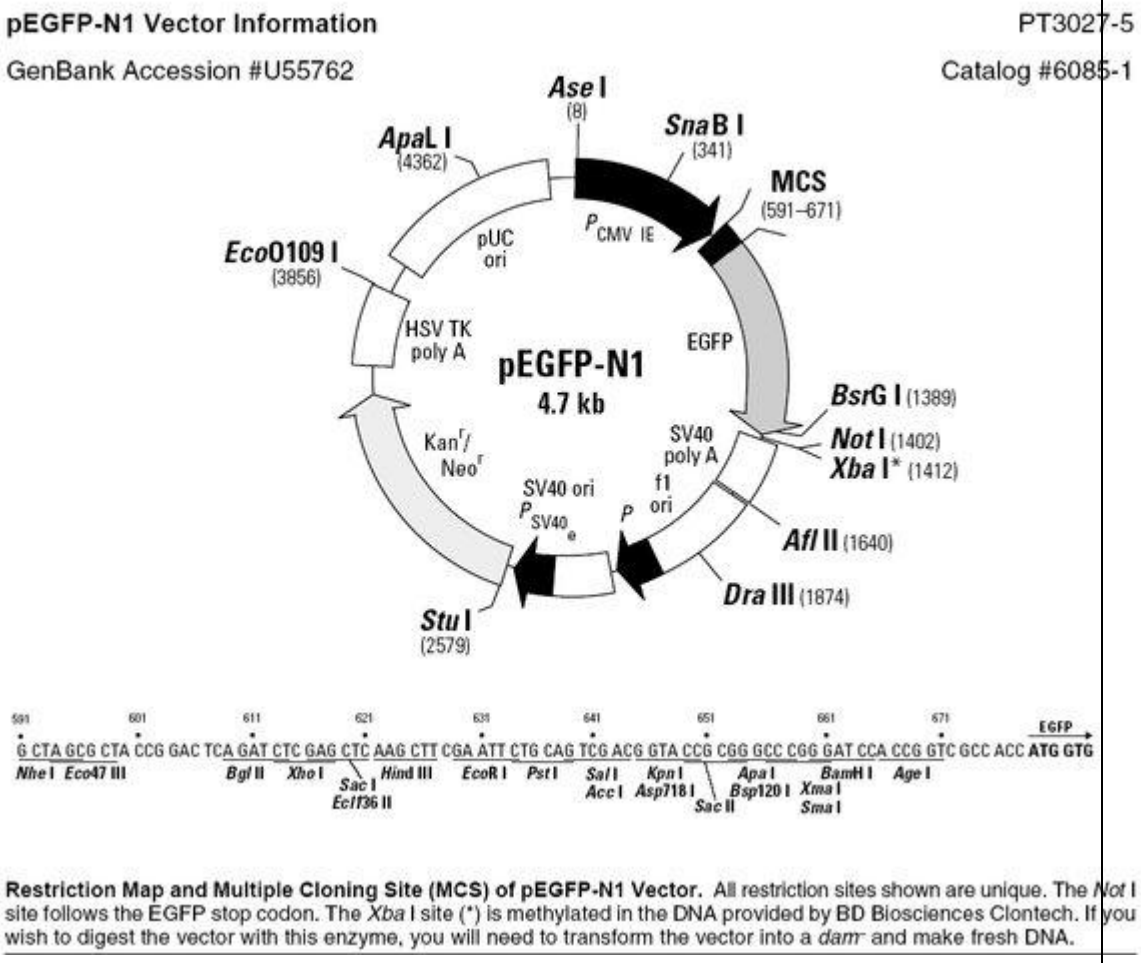

Restriction Map and Multiple Cloning Site (MCS) of pEGFP-N1 Vector. All restriction sites shown are unique. The *Not* I site follows the EGFP stop codon. The *Xba* I site (*) is methylated in the DNA provided by BD Biosciences Clontech. If you wish to digest the vector with this enzyme, you will need to transform the vector into a *dam*⁻ and make fresh DNA.

Figure 21. **Plasmid map of pEGFP-N1**

6.2.2 Primers

Gene	Primer	Sequence (5'-3')
18s	Forward	CGATGCTCTTAGCTGAGTGT
	Reverse	GGTCCAAGAATTTCACCTCT
PS2	Forward	TCGCCTTTGGAGCAGAGAGGA
	Reverse	CACCAGGAAAACCACAATTCT
GAP-DH	Forward	GAAGGTGAAGGTCGGAGTC
	Reverse	GAAGATGGTGATGGCATTTC

6.3 APPENDIX 3

6.3.1 Methods section elaborated

6.3.1.1 Preparation of different drug concentrations

Treatment conditions for RNA assay

1. Vehicle 0µM
2. 4-OH TAM 0.1µM
3. 4-OH TAM 0.5µM
4. 4-OH TAM 1µM

Calculated Volumes: 2ml per well x 4 wells = 8 mls per drug condition

- 0µM dose = 8mls DCC media + 8ul of EtOH
- 0.1µM dose = 8mls DCC media + 8ul of 0.1mM 4OHTAM
- 0.5µM dose = 8mls DCC media + 8ul of 0.5mM 4OHTAM
- 1µM dose = 8mls DCC media + 8ul of 1mM 4OHTAM

Applied volume = 2mL per well so we have excess for pipetting.

Treatment conditions for growth assay

1. Vehicle 0µM
2. 4-OH TAM 0.05µM
3. 4-OH TAM 0.1µM
4. 4-OH TAM 0.5µM
5. 4-OH TAM 1µM

Calculated Volumes: 0.2ml per well x 12 wells = 2.4 mls per drug condition

0µM dose = 2.4 mL DCC media + 2.4ul of EtOH

0.05µM dose = 2.4 mL DCC media + 2.4ul of 0.05mM 4OHTAM

0.1µM dose = 2.4 mL DCC media + 2.4ul of 0.1mM 4OHTAM

0.5µM dose = 2.4 mL DCC media + 2.4ul of 0.5mM 4OHTAM

1µM dose= 2.4 mL DCC media + 2.4ul of 1mM 4OHTAM

Applied volume = 0.15mL (150µL) per well so we have excess for pipetting.

6.3.1.2 From Luciferase assay calculation

	amount(ug)	conc (ug/ul)	vol (ul)	lipofectamine (1:2)	SF Phenol red RPMI (ul)
ERE-TK-Luc [firefly]	1.36	173	8		
pRLNull [Renilla]	0.136	83	1.6		60
				2.7ul	60
Tube A	8ul ERE-TK-Luc+ 1.6ul pRNull		60ul SF RPMI		
Tube B	2.7ul Lipofectamine		60ul SF RPMI		
Incubate 5 mins					
Combine A+B. Then incubate 20 mins.					
Add 560ul SF RPMI to make upto total of 680ul enough for 68 wells.					
Pippette 10ul into each well on top of the stripped media.					

6.3.2 Results section elaborated

6.3.2.1 Input code used in R studio to analyse results using ANOVA followed by a Tukey HSD post-hoc test, comparing each dose to one another between the IRES and UGT2B15 cell lines.

Input code:

```
# read the csv file containing the correctly formated data into R as a dataframe
df <- read.csv("CVA 4 expts combined.csv")
df <- data.frame( CellLine = c(rep("IRES", 20), rep("2B15", 20)), Dose = rep(c(0, 0.05,
0.1, 0.5, 1), 8), Response = c(1.0000000, 0.7593897, 0.7323944, 0.6798976,
0.6032864, 1.0000000, 0.7259615, 0.6410256, 0.6089744, 0.3317308, 0.9972222,
0.5277778, 0.6138889, 0.5750000, 0.4444444, 0.9996305, 0.5321508, 0.5968219,
0.4526977, 0.4194383, 1.0000000, 0.8236715, 0.8236715, 0.7657005, 0.6026570,
1.0000000, 0.8986254, 0.8865979, 0.8556701, 0.3625430, 1.0000000, 1.1874623,
0.7414105, 0.7052441, 0.8951175, 1.0000000, 1.1874623, 0.7414105, 0.7052441,
0.8951175))
#set the Cellline column as a factor
df$CellLine <- as.factor(df$CellLine)
#set the Dose column column as a factor
df$Dose <- as.factor(df$Dose)
#Run the aov function using the df  dataframe
result <- aov(Response ~ CellLine * Dose, data = df)
#Run the TukeyHSD function using the result
posthoc <- TukeyHSD(result, "CellLine:Dose")
#print the output
print(posthoc)
```

6.3.2.2 Cutoff values used for significance analysis

Table 6. Cutoff values indicating increasing significance for statistical analysis

Cutoff values for significance	
0.05	*
0.01	**
0.005	***
0.001	***

6.3.2.3 Data collected from R program by comparing the growth response at each TAM dose to the vehicle (untreated condition) against each cell line independently

Comparing the growth response at each TAM dose to the untreated (Vehicle) for each cell line independe					
IRES:0.05-IRES:0	-0.362893225	-0.6617759	-0.064010523	0.0083227	**
IRES:0.1-IRES:0	-0.353180475	-0.6520632	-0.054297773	0.0110584	*
IRES:0.5-IRES:0	-0.420070750	-0.7189535	-0.121188048	0.0014778	***
IRES:1-IRES:0	-0.549488200	-0.8483709	-0.250605498	0.0000259	****
2B15:0.05-2B15:0	0.024305375	-0.2745773	0.323188077	0.9999997	
2B15:0.1-2B15:0	-0.201727400	-0.5006101	0.097155302	0.4162047	
2B15:0.5-2B15:0	-0.242035300	-0.5409180	0.056847402	0.1950260	
2B15:1-2B15:0	-0.311141250	-0.6100240	-0.012258548	0.0360718	*

Comparing the growth response between the IRES and the 2B15 cell lines at each TAM dose					
IRES:0-2B15:0	-0.000786825	-0.2996695	0.298095877	1.0000000	
IRES:0.05-2B15:0.05	-0.387985425	-0.6868681	-0.089102723	0.0039371	***
IRES:0.1-2B15:0.1	-0.152239900	-0.4511226	0.146642802	0.7661996	
IRES:0.5-2B15:0.5	-0.178822275	-0.4777050	0.120060427	0.5791965	
IRES:1-2B15:1	-0.239133775	-0.5380165	0.059748927	0.2073324	

6.3.2.4 *Input code used in R studio to analyse results using ANOVA followed by a Tukey HSD post-hoc test, conducted on the qRT-PCR data from gene expression analysis.*

R-code for ANOVA and HSD and Output

code

```
install.packages("tidyverse")
# Load necessary packages
library(tidyverse)
library(car)  # for Anova()

# Assuming your data is in a data frame called df
# Make sure Dose is treated as a factor if it's categorical
df <- df %>% rename(Cell_Line = `Cell Line`) %>% mu
drop_na(Response)
# Run two-way ANOVA
anova_model <- aov(Response ~ Cell_Line * Dose, dat
# Summary of the ANOVA
summary(anova_model)
posthoc <- TukeyHSD(anova_model, "Cell_Line:Dose")
print(posthoc)
```

6.3.2.5 *Output generated from R studio by comparing gene expression levels of each cell lines at each of the studied doses of 4-OH-TAM*

Output

```
summary(anova_model)
               Df Sum Sq Mean Sq F value Pr(>F)
Cell_Line       1 0.0554  0.0554   0.394 0.5384
Dose            3 1.8842  0.6281   4.471 0.0173 *
Cell_Line:Dose  3 0.2215  0.0738   0.526 0.6705
Residuals      17 2.3881  0.1405
---
Signif. codes:  0 ‘***’ 0.001 ‘**’ 0.01 ‘*’ 0.05 ‘.’ 0.1 ‘ ’
1


Tukey multiple comparisons of means
    95% family-wise confidence level

Fit: aov(formula = Response ~ Cell_Line * Dose, data = df)

$`Cell_Line:Dose`
                            diff        lwr       upr     p adj
IRES:0-2B15:0     -4.440892e-16 -0.9103896 0.9103896 1.0000000
2B15:0.1-2B15:0    1.816440e-01 -0.9333510 1.2966389 0.9989727
IRES:0.1-2B15:0    4.610575e-01 -0.6539374 1.5760525 0.8360407
2B15:0.5-2B15:0   -3.276112e-01 -1.3109443 0.6557219 0.9370443
IRES:0.5-2B15:0   -4.356191e-01 -1.4189522 0.5477140 0.7863243
2B15:1-2B15:0     -6.075073e-01 -1.5908404 0.3758258 0.4397350
IRES:1-2B15:0     -2.590066e-01 -1.1693962 0.6513829 0.9718276
2B15:0.1-IRES:0    1.816440e-01 -0.9333510 1.2966389 0.9989727
IRES:0.1-IRES:0    4.610575e-01 -0.6539374 1.5760525 0.8360407
2B15:0.5-IRES:0   -3.276112e-01 -1.3109443 0.6557219 0.9370443
IRES:0.5-IRES:0   -4.356191e-01 -1.4189522 0.5477140 0.7863243
2B15:1-IRES:0     -6.075073e-01 -1.5908404 0.3758258 0.4397350
IRES:1-IRES:0     -2.590066e-01 -1.1693962 0.6513829 0.9718276
IRES:0.1-2B15:0.1  2.794136e-01 -1.0080717 1.5668988 0.9939291
2B15:0.5-2B15:0.1 -5.092552e-01 -1.6845630 0.6660527 0.8033171
IRES:0.5-2B15:0.1 -6.172631e-01 -1.7925709 0.5580448 0.6258200
2B15:1-2B15:0.1   -7.891513e-01 -1.9644591 0.3861566 0.3441941
IRES:1-2B15:0.1   -4.406506e-01 -1.5556455 0.6743444 0.8637600
2B15:0.5-IRES:0.1 -7.886687e-01 -1.9639766 0.3866391 0.3448748
IRES:0.5-IRES:0.1 -8.966766e-01 -2.0719845 0.2786312 0.2141973
2B15:1-IRES:0.1   -1.068565e+00 -2.2438727 0.1067430 0.0898361
IRES:1-IRES:0.1   -7.200642e-01 -1.8350591 0.3949308 0.3882682
IRES:0.5-2B15:0.5 -1.080079e-01 -1.1592352 0.9432194 0.9999509
2B15:1-2B15:0.5   -2.798961e-01 -1.3311234 0.7713312 0.9803331
IRES:1-2B15:0.5    6.860458e-02 -0.9147285 1.0519377 0.9999965
2B15:1-IRES:0.5   -1.718882e-01 -1.2231155 0.8793391 0.9989482
IRES:1-IRES:0.5    1.766125e-01 -0.8067206 1.1599456 0.9980947
IRES:1-2B15:1      3.485007e-01 -0.6348324 1.3318338
0.9156830
```

Note: Anova showed that dose was a significant factor. But The Tukey post hoc test found no significant difference between any pair of conditions. "This is likely because:

- Small sample size: Not enough power to detect pairwise differences.
- High within-group variability: If responses vary a lot within each dose group, it's harder to detect differences between them.
- Effect is spread across multiple groups: The overall trend might be significant (e.g., increasing or decreasing response with dose), but no two doses are far enough apart to be significant on their own."

6.3.2.6 Data used to generate figure 13 under results section 3.3

Table 7. Quantitative measurement of UGT2B15 mRNA overexpression in transiently transfected MCF7 cell lines across 3 independent experiments

Experiment number	Cell line type	gapdh (average mRNA level)	2B15 (average mRNA level)	dCt	power Ct	power dCT	UGT2B15 over expression (fold IRES transfected)
Expt1	IRES	15.415	30.85	15.435	0.516683549	2.3	1.00
	UGT2B15	16.395	24.19	7.795	52.24977263	450.3	199.47
Expt 2	IRES	12.83	25.65	12.82	18.99243336	13.8	1.00
	UGT2B15	12.71	22.57	9.86	160.6027576	107.6	7.78
Expt 3	IRES	13.635	25.62	11.985	19.39150476	24.7	1.00
	UGT2B15	14.23	23.12	8.89	109.6949161	210.8	8.54

6.3.3 Supplemental material

6.3.3.1 Confirmation of UGT2B17 expression in previously established ZR75 stable cell lines by Immunoblotting

For future assays, ZR75 stable cell lines were also recovered from cryopreservation and validated using the western blot technique.

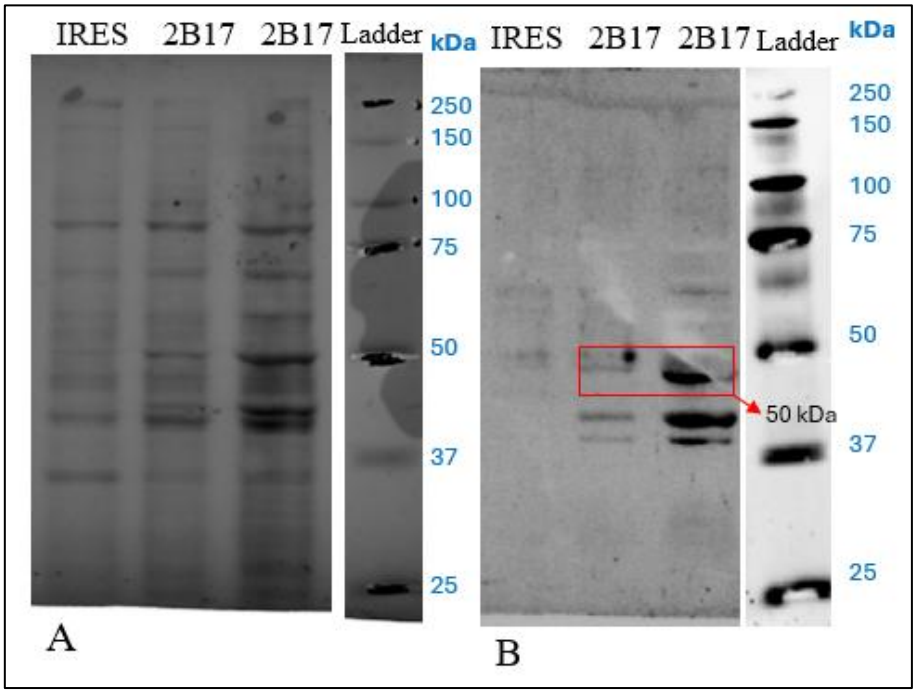

Figure 22. **Analysis of UGT2B17 protein expression in ZR75 stable cell lines by using Immunoblotting technique.**

(A) Image depicting protein from ZR75 -IRES and 2 independent ZR75-2B17 stable cell lines separated in SDS-PAGE and stained with Ponceau red.(Akhdar et al.) Western blot image of the same samples probes with anti-UGT2B15/17. The band at approximately 50kDa marked in a red box indicated by arrow appeared in ZR75-2B17 cell lines and not in ZR75-IRES, confirming the integration of UGT2B15 construct in the cell type under study. Protein ladder is shown at the right end of the gel images with the sizes marked in blue for size reference.